Bioorg. Med. Chem. 95 (2023) 117510

Contents lists available at ScienceDirect

Bioorganic & Medicinal Chemistry

journal homepage: www.elsevier.com/locate/bmc

Synthesis, anti-inflammatory activity, inverse molecular docking, and acid dissociation constants of new naphthoquinone-thiazole hybrids

Cagla Efeoglu [a], Sena Taskin [b], Ozge Selcuk [a], Begum Celik [c,d], Ece Tumkaya [c,d], Abdulilah Ece [e,*], Hayati Sari [f], Zeynel Seferoglu [g], Furkan Ayaz [h,*], Yahya Nural [a,*]

[a] Department of Analytical Chemistry, Faculty of Pharmacy, Mersin University, Mersin TR-33169, Türkiye
[b] Department of Analytical Chemistry, Faculty of Pharmacy, Biruni University, İstanbul 34010, Türkiye
[c] Department of Biotechnology, Faculty of Arts and Science, Mersin University, TR-33440 Mersin, Türkiye
[d] Mersin University Biotechnology Research and Application Center, Mersin University, TR-33440 Mersin, Türkiye
[e] Department of Pharmaceutical Chemistry, Faculty of Pharmacy, Biruni University, İstanbul 34010, Türkiye
[f] Department of Chemistry, Faculty of Science and Arts, Gaziosmanpasa University, 60250 Tokat, Türkiye
[g] Department of Chemistry, Faculty of Science, Gazi University, TR-06560 Ankara, Türkiye
[h] Department of Molecular Biology and Genetics, Faculty of Engineering and Natural Sciences, Biruni University, İstanbul 34010, Türkiye

ARTICLE INFO

Keywords:
Anti-inflammatory activity
Inverse molecular docking
Naphthoquinone
Thiazole
Acid dissociation constants

ABSTRACT

Chronic Inflammation is associated with various types of diseases that involves pro-inflammatory cytokines like IL-6 and TNF-α. High costs and serious side effects of available anti-inflammatory/immunomodulatory drugs led us to design new compounds with promising anti-inflammatory activities. Many drugs and biologically important compounds involve naphthoquinone and thiazole moieties in their core structures. Thereby, here we report the synthesis, characterization and anti-inflammatory activities of new naphthoquinone thiazole hybrids by reaction of naphthoquinone acyl thioureas with various α-bromoketone derivatives. The position of NO_2 group in one of the phenyl rings of naphthoquinone thiazole hybrids was changed while different substituents were introduced at the para position of the second phenyl ring. All compounds were tested for potential immunomodulatory effect. No inflammatory cytokines were observed in the absence of LPS stimulant. On the other hand, they had promising anti-inflammatory immunomodulatory activities by being able to decrease the production of the pro-inflammatory cytokines (TNF-α and IL-6) in the LPS-stimulated cells. In an effort to find the possible mechanism of action, several enzymes involved in signalling pathways that play critical roles in inflammatory responses were screened *in silico*. Subsequent to inverse molecular docking approach, PI3K was predicted be the potential target. The docked complexes of the most potent compounds **5g** and **5i** were subjected to molecular dynamics simulation to assess the binding stability of the igands with the putative target. Acid dissociation constants (pK_a) of the products were also determined potentiometrically.

1. Introduction

Since most drug molecules contain heteroatoms such as nitrogen, oxygen, and sulfur, pharmacophore groups bearing such atoms have been intensively studied in medicinal chemistry.[1–4] Naphthoquinone moiety is a privileged heterocyclic pharmacophore involved in many synthetic or naturally occurring pharmaceutically active compounds such as doxorubicin, atovaquone, plumbagin, and vitamin K_3.[5,6] Recent studies have shown that compounds bearing naphthoquinone scaffold exhibit a wide range of pharmacological activities including anti-cancer,[7,8] DNA binding/cleavage,[9] antileishmanial, anti-mycobacterial,[10] antibacterial and antifungal[9] activity as well as carbonic anhydrase[11] and acetylcholinesterase[12] inhibition activities.

Designing and synthesizing heterocyclic moieties as a pharmacophore group constitute an important part of drug research studies and several studies have reported many heterocyclic scaffolds in this context.[13–16] Among these structures, thiazole ring, a five-membered heterocyclic structure containing sulfur and nitrogen atoms, has a very

* Corresponding authors at: Department of Analytical Chemistry, Faculty of Pharmacy, Mersin University, Mersin TR-33169, Türkiye (Y. Nural); Department of Pharmaceutical Chemistry, Faculty of Pharmacy, Biruni University, İstanbul 34010, Türkiye (A. Ece); Department of Molecular Biology and Genetics, Faculty of Engineering and Natural Sciences, Biruni University, İstanbul, 34010, Türkiye (F. Ayaz).
E-mail addresses: aece@biruni.edu.tr (A. Ece), fayaz@biruni.edu.tr (F. Ayaz), yahyanural@mersin.edu.tr (Y. Nural).

https://doi.org/10.1016/j.bmc.2023.117510
Received 6 October 2023; Received in revised form 26 October 2023; Accepted 30 October 2023
Available online 31 October 2023

important place in drug research. As of today, many drugs available at the markets such as Ritonavir, Abafungin, and Tiazofurin[17,18] have a thiazole ring in their scaffold. In recent years, the synthesis of hybrid molecules has been carried out intensively for the synthesis of more potent compounds and various papers have reported hybrid molecules containing thiazole show broad spectrum bioactivities such as antimicrobial,[19–21] anticancer,[22,23] DNA cleavage, antioxidant,[24] and anticonvulsant[25] activities as well as α-amylase,[26] aromatase,[27] and dihydrofolate reductase[28] enzyme inhibitor activities.

Inflammation is present in a vast range of physiological and pathological processes[29] and many natural compounds and their derivatives have been investigated for their anti-inflammatory activities.[5,30] New naphthoquinone-thiazole hybrid compounds were designed in this study due to the presence of many 1,4-naphthoquinone[31–36] or thiazole[17,37–43] derivatives with anti-inflammatory effects as well as many other different bioactivities mentioned above. As a specific example, a non-steroidal anti-inflammatory drug Fentiazac is a thiazole-based compound. Vitamin K_3, shikonin and plumbagin contain napththoquinone core and have also been reported to have anti-inflammatory properties.[44] Since the synthesis of hybrids containing multiple pharmacophore groups has become an important strategy to achieve invaluable pharmacological activities, we aimed to design naphthoquinone-thiazole hybrids to achieve better anti-inflammatory activity.

Non-steroidal anti-inflammatory drug candidates are needed in the field to diversify our arsenal against inflammatory disorders.[45] In our study, we focused on macrophages that have been heavily associated with inflammatory responses in different diseases.[46] These cells are unique in a way that they bridge different immune system cells and their responses. They can produce cytokines to define or shape the type of immune response.[47] In our *in vitro* model of inflammation, macrophages were stimulated by LPS from Gram-negative bacteria to measure the changes in the production levels of two major inflammatory cytokines: TNFα and IL6. The anti-inflammatory potentials of the designed naphthoquinone-thiazole hybrids were tested on the LPS-activated macrophages.[48–50]

Here, twelve new naphthoquinone thiazole compounds were synthesized and to compare the structure and anti-inflammatory activity relationship of those hybrids, the position of the NO_2 group in a phenyl ring was changed while the substituent at the para position of the other phenyl ring was altered with F, Cl or Br. In order to provide mechanistic insights into potential inhibition profiles of the compounds, we employed inverse docking approach to find out possible biological target and then, we carried out molecular dynamics simulations to assess stability and dynamics of ligand–protein complexes. Since acid dissociation constant (pK_a) provides information about the acidity, solubility, and many other properties of compounds, pK_a values of the products in dimethyl sulfoxide (DMSO):water (20:80 *v/v*) are also reported.

2. Experimental

2.1. Synthesis of 1,4-naphthoquinone acyl thiourea derivatives, 3a–c

The 1,4-naphthoquinone acyl thiourea derivatives **3a–c** were prepared by reaction of 2,3-diaminonaphthalene-1,4-dione and corresponding acyl isothiocyanate in acetone at reflux temperature as described previously.[51]

2.2. General procedure for the synthesis of naphthoquinone thiazole hybrids, 5a–l

A stirred solution of naphthoquinone acyl thiourea (1 mmol) in acetone (50 mL) was stirred under reflux temperature for 15 min. Then, a solution of corresponding 2-bromo-1-substituted ethanone (1.2 mmol) in acetone (30 mL) was added dropwise to the naphthoquinone acyl thiourea mixture which was stirred under reflux temperature. In the reaction follow-up with TLC, it was determined that the reactions were completed in 24 h, 36 h, and 72 h, for the compounds **5a–d**, **5e–h**, and **5i–l**, respectively. After the reaction was completed, the acetone was completely evaporated under reduced pressure and the crude mixture was washed with diethyl ether and then several times with methanol. Molecular structures of the pure products obtained **5a–l** were characterized using FT-IR, HRMS, ^{1}H NMR, ^{13}C NMR (Figs. S1–S48), and elemental analysis.

2.2.1. N-(3-(3-amino-1,4-dioxo-1,4-dihydronaphthalen-2-yl)-4-phenylthiazol-2(3H)-ylidene)-4-nitrobenzamide, 5a

Yellow powder. Yield, 0.44 g, 89 %. m.p.: 287–289 °C (decomp.). IR (cm^{-1}): υ_{max} 3438, 3285, 3250, 3143, 1684, 1666, 1648, 1622, 1563, 1509, 1450, 1441, 1404, 1331, 1262. Anal. Calc. for $C_{26}H_{16}N_4O_5S$: C, 62.90; H, 3.25; N, 11.28; S, 6.46. Found: C, 62.97; H, 3.22; N, 11.05; S, 6.40 %. ^{1}H NMR (400 MHz, DMSO-d_6): δ 8.31 (s 1H, NH), 8.22–8.19 (m, 4H, Ar—H and N—H), 8.08–8.06 (m, 1H, Ar—H), 7.86–7.75 (m, 4H, Ar—H), 7.36–7.32 (m, 5H, Ar—H), 7.26 (s, 1H, thiazole C—H). ^{13}C NMR (100 MHz, DMSO-d_6): δ 180.9 (C═O), 175.9 (C═O), 171.1 (C═O), 170.1. 149.1, 147.1, 142.4, 139.7, 135.6, 132.9, 131.7, 130.3, 130.0, 129.8 (2 × C), 129.3, 128.3 (2 × C), 128.0 (2 × C), 126.5, 125.9, 123.5 (2 × C), 112.0, 108.0. HRMS (ESI-TOF-MS): calcd. for $C_{26}H_{17}N_4O_5S$ $[MH]^+$ 497.0914; found 497.0912.

2.2.2. N-(3-(3-amino-1,4-dioxo-1,4-dihydronaphthalen-2-yl)-4-(4-fluorophenyl)thiazol-2(3H)-ylidene)-4-nitrobenzamide, 5b

Orange powder. Yield, 0.43 g, 84 %. m.p.: 301–303 °C (decomp.). IR (cm^{-1}): υ_{max} 3440, 3289, 3255, 3113, 1683, 1666, 1651, 1626, 1610, 1578, 1567, 1504, 1454, 1400, 1330, 1264. Anal. Calc. for $C_{26}H_{15}FN_4O_5S$: C, 60.70; H, 2.94; N, 10.89; S, 6.23. Found: C, 61.06; H, 2.95; N, 10.95; S, 6.15 %. ^{1}H NMR (400 MHz, DMSO-d_6): δ 8.33 (s 1H, NH), 8.23–8.22 (m, 4H, Ar—H and N—H), 8.09–8.07 (m, 1H, Ar—H), 7.88–7.77 (m, 4H, Ar—H), 7.41–7.37 (m, 2H, Ar—H), 7.28 (s, 1H, thiazole C—H), 7.24–7.19 (m, 2H, Ar—H). ^{13}C NMR (100 MHz, DMSO-d_6): δ 180.8 (C═O), 175.9 (C═O), 171.2 (C═O), 170.0, 162.5 (d, J_{FC} = 246.8 Hz, C-F), 149.2, 147.2, 142.3, 138.6, 135.5, 132.9, 131.7, 130.3 (d, J_{FC} = 8.6 Hz, 2 × C), 130.0, 129.8 (2 × C), 126.7 (d, J_{FC} = 3.1 Hz), 126.5, 125.9, 123.5 (2 × C), 115.4 (d, J_{FC} = 21.9 Hz, 2 × C), 111.7, 108.2. HRMS (ESI-TOF-MS): calcd. for $C_{26}H_{16}FN_4O_5S$ $[MH]^+$ 515.0820; found 515.0812.

2.2.3. N-(3-(3-amino-1,4-dioxo-1,4-dihydronaphthalen-2-yl)-4-(4-chlorophenyl)thiazol-2(3H)-ylidene)-4-nitrobenzamide, 5c

Orange powder. Yield, 0.48 g, 90 %. m.p.: 309–311 °C (decomp.). IR (cm^{-1}): υ_{max} 3438, 3288, 3246, 3109, 1683, 1666, 1650, 1626, 1577, 1568, 1532, 1514, 1486, 1463, 1454, 1400, 1367, 1330, 1264. Anal. Calc. for $C_{26}H_{15}ClN_4O_5S$: C, 58.82; H, 2.85; N, 10.55; S, 6.04. Found: C, 58.73; H, 2.94; N, 10.36; S, 5.95 %. ^{1}H NMR (400 MHz, DMSO-d_6): δ 8.31 (s 1H, NH), 8.23–8.19 (m, 4H, Ar—H and N—H), 8.09–8.06 (m, 1H, Ar—H), 7.87–7.77 (m, 4H, Ar—H), 7.45–7.35 (m, 4H, Ar—H), 7.30 (s, 1H, thiazole C—H). ^{13}C NMR (100 MHz, DMSO-d_6): δ 180.8 (C═O), 175.9 (C═O), 171.2 (C═O), 170.0, 149.2, 147.2, 142.3, 138.5, 135.5, 134.0, 132.9, 131.7, 130.0, 129.8 (2 × C), 129.7 (2 × C), 129.1, 128.5 (2 × C), 126.5, 125.9, 123.5 (2 × C), 111.6, 108.6. HRMS (ESI-TOF-MS): calcd. for $C_{26}H_{16}ClN_4O_5S$ $[MH]^+$ 531.0524; found 531.0510.

2.2.4. N-(3-(3-amino-1,4-dioxo-1,4-dihydronaphthalen-2-yl)-4-(4-bromophenyl)thiazol-2(3H)-ylidene)-4-nitrobenzamide, 5d

Yellow powder. Yield, 0.53 g, 92 %. m.p.: 318–320 °C (decomp.). IR (cm^{-1}): υ_{max} 3410, 3288, 3255, 3111. 3096, 1683, 1666, 1649, 1625, 1575, 1564, 1516, 1485, 1455, 1399, 1368, 1331, 1262. Anal. Calc. for $C_{26}H_{15}BrN_4O_5S$: C, 54.27; H, 2.63; N, 9.74; S, 5.57. Found: C, 54.62; H, 2.63; N, 9.66; S, 5.66 %. ^{1}H NMR (400 MHz, DMSO-d_6): δ 8.33 (s 1H, NH), 8.24–8.19 (m, 4H, Ar—H and N—H), 8.10–8.08 (m, 1H, Ar—H), 7.89–7.77 (m, 4H, Ar—H), 7.58–7.56 (m, 2H, Ar—H), 7.32–7.31 (m, 2H, Ar—H), 7.29 (s, 1H, thiazole C—H). ^{13}C NMR (100 MHz, DMSO-d_6): δ 180.7 (C═O), 175.9 (C═O), 171.2 (C═O), 170.0, 149.2, 147.2, 142.3,

138.5, 135.5, 132.9, 131.7, 131.5 (2 × C), 130.04, 129.95 (2 × C), 129.8 (2 × C), 129.5, 126.5, 125.9, 123.5 (2 × C), 112.7, 111.6, 108.0. HRMS (ESI-TOF-MS): calcd. for $C_{26}H_{16}BrN_4O_5S$ $[MH]^+$ 575.0019; found 575.0008.

2.2.5. N-(3-(3-amino-1,4-dioxo-1,4-dihydronaphthalen-2-yl)-4-phenylthiazol-2(3H)-ylidene)-3-nitrobenzamide, **5e**

Orange powder. Yield, 0.42 g, 85 %. m.p.: 315–317 °C (decomp.). IR (cm^{-1}): υ_{max} 3439, 3366, 3285, 3255, 3116, 1686, 1647, 1613, 1575, 1558, 1530, 1510, 1455, 1366, 1332, 1262. Anal. Calc. for $C_{26}H_{16}N_4O_5S$: C, 62.90; H, 3.25; N, 11.28; S, 6.46. Found: C, 62.65; H, 3.20; N, 11.42; S, 6.35 %. ^{1}H NMR (400 MHz, DMSO-d_6): δ 8.73 (s, 1H, Ar—H), 8.39–8.28 (m, 2H, Ar—H), 8.32 (s 1H, NH), 8.09 (d, 1H, J = 7.2 Hz, Ar—H), 7.87–7.77 (m, 4H, Ar—H and N—H), 7.71–7.67 (m, 1H, Ar—H), 7.37–7.34 (m, 5H, Ar—H), 7.25 (s, 1H, thiazole C—H). ^{13}C NMR (100 MHz, DMSO-d_6): δ 180.9 (C═O), 176.0 (C═O), 170.7 (C═O), 169.9, 147.8, 147.1, 139.7, 138.4, 135.6, 134.5, 132.9, 131.8, 130.2, 130.0, 129.9, 129.2, 128.4 (2 × C), 127.9 (2 × C), 126.4, 125.9, 125.8, 123.1, 112.0, 107.8. HRMS (ESI-TOF-MS): calcd. for $C_{26}H_{17}N_4O_5S$ $[MH]^+$ 497.0914; found 497.0909.

2.2.6. N-(3-(3-amino-1,4-dioxo-1,4-dihydronaphthalen-2-yl)-4-(4-fluorophenyl)thiazol-2(3H)-ylidene)-3-nitrobenzamide, **5f**

Yellow powder. Yield, 0.41 g, 80 %. m.p.: 328–330 °C (decomp.). IR (cm^{-1}): υ_{max} 3374, 3296, 3255, 3112, 1694, 1670, 1649, 1611, 1590, 1575, 1558, 1530, 1515, 1455, 1406, 1333, 1264. Anal. Calc. for $C_{26}H_{15}FN_4O_5S$: C, 60.70; H, 2.94; N, 10.89; S, 6.23. Found: C, 60.95; H, 2.90; N, 10.73; S, 6.36 %. ^{1}H NMR (400 MHz, DMSO-d_6): δ 8.73 (s, 1H, Ar—H), 8.39–8.29 (m, 2H, Ar—H), 8.35 (s 1H, NH), 8.10 (d, 1H, J = 7.0 Hz, Ar—H), 7.90–7.78 (m, 4H, Ar—H and N—H), 7.71–7.67 (m, 1H, Ar—H), 7.42–7.39 (m, 2H, Ar—H), 7.27 (s, 1H, thiazole C—H), 7.25–7.20 (m, 2H, Ar—H). ^{13}C NMR (100 MHz, DMSO-d_6): δ 180.8 (C═O), 176.0 (C═O), 170.7 (C═O), 169.8, 162.5 (d, J_{FC} = 246.8 Hz, C-F), 147.8, 147.2, 138.6, 138.4, 135.5, 134.5, 132.9, 131.8 130.3 (d, J_{FC} = 8.6 Hz, 2 × C), 130.03, 129.97, 126.7 (d, J_{FC} = 2.8 Hz), 126.4, 125.90, 125.86, 123.1, 115.5 (d, J_{FC} = 21.9 Hz, 2 × C), 111.7, 108.0. HRMS (ESI-TOF-MS): $C_{26}H_{16}FN_4O_5S$ $[MH]^+$ 515.0820; found 515.0813.

2.2.7. N-(3-(3-amino-1,4-dioxo-1,4-dihydronaphthalen-2-yl)-4-(4-chlorophenyl)thiazol-2(3H)-ylidene)-3-nitrobenzamide, **5g**

Yellow powder. Yield, 0.47 g, 89 %. m.p.: 336–338 °C (decomp.). IR (cm^{-1}): υ_{max} 3375, 3290, 3255, 3112, 1692, 1670, 1648, 1610, 1589, 1575, 1552, 1529, 1515, 1452, 1406, 1332, 1265. Anal. Calc. for $C_{26}H_{15}ClN_4O_5S$: C, 58.82; H, 2.85; N, 10.55; S, 6.04. Found: C, 58.95; H, 2.84; N, 10.72; S, 6.10 %. ^{1}H NMR (400 MHz, DMSO-d_6): δ 8.73 (s, 1H, Ar—H), 8.39–8.29 (m, 2H, Ar—H), 8.35 (s 1H, NH), 8.10 (d, 1H, J = 7.1 Hz, Ar—H), 7.92–7.78 (m, 4H, Ar—H and N—H), 7.71–7.67 (m, 1H, Ar—H), 7.46–7.44 (m, 2H, Ar—H), 7.39–7.36 (m, 2H, Ar—H), 7.31 (s, 1H, thiazole C—H). ^{13}C NMR (100 MHz, DMSO-d_6): δ 180.8 (C═O), 175.9 (C═O), 170.7 (C═O), 169.8, 147.8, 147.2, 138.4, 138.3, 135.6, 134.5, 134.0, 133.0, 131.7, 130.1, 130.0, 129.7 (2 × C), 129.1, 128.6 (2 × C), 126.5, 125.9 (2 × C), 123.1, 111.6, 108.4. HRMS (ESI-TOF-MS): calcd. for $C_{26}H_{16}ClN_4O_5S$ $[MH]^+$ 531.0524; found 531.0519.

2.2.8. N-(3-(3-amino-1,4-dioxo-1,4-dihydronaphthalen-2-yl)-4-(4-bromophenyl)thiazol-2(3H)-ylidene)-3-nitrobenzamide, **5h**

Orange powder. Yield, 0.48 g, 84 %. m.p.: 327–329 °C (decomp.). IR (cm^{-1}): υ_{max} 3374, 3296, 3256, 3110, 1683, 1648, 1610, 1589, 1575, 1558, 1529, 1515, 1455, 1403, 1332, 1265. c ^{1}H NMR (400 MHz, DMSO-d_6): δ 8.73–8.72 (m, 1H, Ar—H), 8.39–8.28 (m, 2H, Ar—H), 8.34 (s 1H, NH), 8.11 (dd, 1H, J = 7.2 Hz, 1.0 Hz, Ar—H), 7.90–7.78 (m, 4H, Ar—H and N—H), 7.71–7.67 (m, 1H, Ar—H), 7.60–7.58 (m, 2H, Ar—H), 7.32–7.30 (m, 3H, Ar—H and thiazole C—H). ^{13}C NMR (100 MHz, DMSO-d_6): δ 180.7 (C═O), 175.9 (C═O), 170.7 (C═O), 169.8, 147.8, 147.2, 138.5, 138.3, 135.6, 134.5, 133.0, 131.7, 131.5 (2 × C), 130.1, 130.0, 129.9 (2 × C), 129.4, 126.5, 125.9 (2 × C), 123.1, 122.7, 111.6, 108.4. HRMS (ESI-TOF-MS): calcd. for $C_{26}H_{16}BrN_4O_5S$ $[MH]^+$ 575.0019; found 575.0009.

2.2.9. N-(3-(3-amino-1,4-dioxo-1,4-dihydronaphthalen-2-yl)-4-phenylthiazol-2(3H)-ylidene)-4-chloro-3-nitrobenzamide, **5i**

Orange powder. Yield, 0.39 g, 73 %. m.p.: 305–307 °C (decomp.). IR (cm^{-1}): υ_{max} 3428, 3304, 3255, 3066, 1687, 1651, 1622, 1588, 1532, 1463, 1442, 1403, 1338, 1264, 1265. Anal. Calc. for $C_{26}H_{15}ClN_4O_5S$: C, 58.82; H, 2.85; N, 10.55; S, 6.04. Found: C, 59.05; H, 2.90; N, 10.48; S, 6.02 %. ^{1}H NMR (400 MHz, DMSO-d_6): δ 8.54 (s, 1H, Ar—H), 8.33 (s 1H, NH), 8.23 (d, 1H, J = 7.7 Hz, Ar—H), 8.10 (d, 1H, J = 7.0 Hz, Ar—H), 7.92–7.82 (m, 5H, Ar—H and N—H), 7.38 (s, 5H, Ar—H), 7.29 (s, 1H, thiazole C—H). ^{13}C NMR (100 MHz, DMSO-d_6): δ 180.8 (C═O), 175.9 (C═O), 170.0 (C═O), 169.8, 147.14, 147.10, 139.7, 137.1, 135.6, 133.2, 132.9, 132.1, 131.7, 130.2, 129.9, 129.3, 128.4 (2 × C), 128.0, 127.9 (2 × C), 126.4, 125.9, 125.5, 111.9, 108.0. HRMS (ESI-TOF-MS): calcd. for $C_{26}H_{16}ClN_4O_5S$ $[MH]^+$ 531.0524; found 531.0516.

2.2.10. N-(3-(3-amino-1,4-dioxo-1,4-dihydronaphthalen-2-yl)-4-(4-fluorophenyl)thiazol-2(3H)-ylidene)-4-chloro-3-nitrobenzamide, **5j**

Orange powder. Yield, 0.41 g, 75 %. m.p.: 291–293 °C (decomp.). IR (cm^{-1}): υ_{max} 3384, 3305, 3254, 3072, 1689, 1651, 1615, 1592, 1538, 1504, 1463, 1407, 1335, 1265. Anal. Calc. for $C_{26}H_{14}ClFN_4O_5S$: C, 56.89; H, 2.57; N, 10.21; S, 5.84. Found: C, 56.95; H, 2.66; N, 9.98; S, 5.80 %. ^{1}H NMR (400 MHz, DMSO-d_6): δ 8.51 (d, 1H, J = 1.6 Hz, Ar—H), 8.32 (s 1H, NH), 8.21 (dd, 1H, J = 8.4 Hz, 1.6 Hz, Ar—H), 8.08 (d, 1H, J = 7.2 Hz, Ar—H), 7.87–7.79 (m, 5H, Ar—H and N—H), 7.39 (dd, 2H, J = 8.4 Hz, 5.5 Hz, Ar—H), 7.28 (s, 1H, thiazole C—H), 7.24—7.19 (m, 2H, Ar—H). ^{13}C NMR (100 MHz, DMSO-d_6): δ 180.7 (C═O), 175.9 (C═O), 169.89 (C═O), 169.86, 162.5 (d, J_{FC} = 246.7 Hz, C-F), 147.2 147.1, 138.7, 137.0, 135.6, 133.2, 133.0, 132.1, 131.7, 130.3 (d, J_{FC} = 8.7 Hz, 2 × C), 129.9, 128.1, 126.6 (d, J_{FC} = 3.0 Hz), 126.5, 125.9, 125.5, 115.5 (d, J_{FC} = 21.9 Hz, 2 × C), 111.6, 108.2. HRMS (ESI-TOF-MS): calcd. for $C_{26}H_{15}ClFN_4O_5S$ $[MH]^+$ 549.0430; found 549.0421.

2.2.11. N-(3-(3-amino-1,4-dioxo-1,4-dihydronaphthalen-2-yl)-4-(4-chlorophenyl)thiazol-2(3H)-ylidene)-4-chloro-3-nitrobenzamide, **5k**

Orange powder. Yield, 0.39 g, 70 %. m.p.: 297–299 °C (decomp.). IR (cm^{-1}): υ_{max} 3437, 3374, 3293, 3259, 3105, 1683, 1649, 1611, 1588, 1568, 1532, 1515, 1470, 1455, 1403, 1335, 1264. Anal. Calc. for $C_{26}H_{14}Cl_2N_4O_5S$: C, 55.23; H, 2.50; N, 9.91; S, 5.67. Found: C, 55.00; H, 2.51; N, 10.05; S, 5.75 %. ^{1}H NMR (400 MHz, DMSO-d_6): δ 8.50 (d, 1H, J = 1.9 Hz, Ar—H), 8.33 (s 1H, NH), 8.20 (dd, 1H, J = 8.4 Hz, 2.0 Hz, Ar—H), 8.10–8.07 (m, 1H, Ar—H), 7.91 (s 1H, NH), 7.85–7.78 (m, 4H, Ar—H), 7.45–7.43 (m, 2H, Ar—H), 7.37–7.34 (m, 2H, Ar—H). 7.32 (s, 1H, thiazole C—H). ^{13}C NMR (100 MHz, DMSO-d_6): δ 180.7 (C═O), 175.9 (C═O), 169.9 (C═O and C), 147.2, 147.1, 138.5, 137.0, 135.5, 134.0, 133.2, 133.0, 132.1, 131.7, 130.0, 129.7 (2 × C), 129.0, 128.6 (2 × C), 128.1, 126.5, 125.9, 125.5, 111.5, 108.6. HRMS (ESI-TOF-MS): calcd. for $C_{26}H_{15}Cl_2N_4O_5S$ $[MH]^+$ 565.0135; found 565.0132.

2.2.12. N-(3-(3-amino-1,4-dioxo-1,4-dihydronaphthalen-2-yl)-4-(4-bromophenyl)thiazol-2(3H)-ylidene)-4-chloro-3-nitrobenzamide, **5l**

Orange powder. Yield, 0.49 g, 81 %. m.p.: 280–283 °C (decomp.). IR (cm^{-1}): υ_{max} 3372, 3296, 3253, 3099, 1687, 1647, 1590, 1569, 1532, 1463, 1336, 1263. Anal. Calc. for $C_{26}H_{14}BrClN_4O_5S$: C, 51.21; H, 2.31; N, 9.19; S, 5.26. Found: C, 51.52; H, 2.35; N, 9.20; S, 5.36 %. ^{1}H NMR (400 MHz, DMSO-d_6): δ 8.50 (d, 1H, J = 1.5 Hz, Ar—H), 8.31 (s 1H, NH), 8.20 (dd, 1H, J = 8.4 Hz, 1.6 Hz, Ar—H), 8.09–8.08 (m, 1H, Ar—H), 7.89–7.77 (m, 5H, Ar—H and NH), 7.59–7.56 (m, 2H, Ar—H), 7.32 (s, 1H, thiazole C—H), 7.30–7.28 (m, 2H, Ar—H). ^{13}C NMR (100 MHz, DMSO-d_6): δ 180.7 (C═O), 175.9 (C═O), 169.93 (C═O), 169.92, 147.23, 147.15, 138.6, 137.0, 135.5, 133.3, 133.0, 132.1, 131.7, 131.5 (2 × C), 130.0, 129.9 (2 × C), 129.4, 128.1, 126.5, 125.9, 125.5, 122.7, 111.5, 108.6. HRMS (ESI-TOF-MS): calcd. for $C_{26}H_{15}BrClN_4O_5S$ $[MH]^+$

608.9630; found 608.9616.

2.3. Cell culture

J774.2 macrophage cell line, which is the immune system cell obtained from ATCC, Roswell Park Memorial Institute (RPMI 1640) medium contains 10 % fetal bovine serum, 1 % antibiotic (100 μg/mL penicillin and 100 μg/mL streptomycin) and sodium pyruvate. In this context, an incubator (37 °C, 5 % CO_2) providing suitable conditions for the growth of cells was used. Application of 12 molecules synthesized, LPS and salicylic acid (SA) to J774.2 cells were as follows: Cells containing immune system cell J774.2 macrophage were added to 1 mL (RPMI 1640) medium to 24-well plates. The cells that we added to the plates were incubated in an incubator at 37 °C, 5 % CO_2 providing the appropriate conditions. To examine the production levels of molecules on TNF-α and IL6 cytokines, 12 molecules were applied at concentrations of 1 μg /mL, 2 μg/mL, and 5 μg/mL.

The indicated 12 molecules were examined with and without the addition of lipopolysaccharide (LPS). After J774.2 cells completed the 24 h formation phase under appropriate conditions, their effects were examined by the ELISA method.

2.4. Elisa method

The Sandwich ELISA method was applied to observe the effects of molecules on TNF-α and IL6 cytokines. ELISA kits (BD Biosciences, CA, USA) were used during this experiment and were performed in accordance with the specified instruction manual.

Application of ELISA kits: The first step was performed by transferring specific antibodies recognizing TNF-α and IL6 cytokines (0.5 μg/mL pH = 9.5, 100 μL/well in bicarbonate buffer) into 96-well plates. Specific antibodies recognizing the transferred cytokines were incubated for 12 h. After this time, the solutions in the ELISA plates were poured. Plates were washed by adding 0.05 % Tween 20 PBS. This process was repeated 3 times.

The next step was to add 200 μL of blocking buffer (1 % BSA PBS) to the wells and incubate at 4 °C for the appropriate time. After the incubation phase was completed, the plates were washed 3 times and the washing process was applied. 100 μL samples were added to the washed wells. Samples added to ELISA plates were incubated at 4 °C for 12 h. The washing process was applied 3 times to the plates whose incubation stage was completed.

In the next step, 100 μL of TNF-α and specific antibodies recognizing IL6 cytokines (0.5 μg/mL in 10 % FBS PBS) were added to the wells. Specific antibodies recognizing the cytokines added to the ELISA plates were incubated within 1 h at the appropriate temperature (room temperature). After the incubation was completed, the solution on the plates was poured out. Afterwards, the plates were washed 3 times.

The incubation process was started by adding 100 μL of Streptavidin HRP solution to the plates that were washed. Incubation was completed within 1 h at room temperature. The ELISA plates, which had completed the incubation process at room temperature, were washed 3 times. Then, 100 μL of TMB substrate (BD OptEIA) was added to the plates. Sulphuric acid (50 μL 1 M) was applied to the wells of the plates to stop the reactions. Absorbance measurement at 450 nm was performed to calculate TNF-α and IL6 concentration levels.

2.5. Cell count

First, supernatants were separated from the wells of the plates, and then the cells were washed with PBS. Trypan blue was added to count the cells and cell viability was determined.

2.6. Inverse molecular docking and molecular dynamics studies

Schrödinger software[52] and related modules were used in *in silico* calculations. High resolution structures of potential proteins were downloaded from protein databank and subjected to protein preparation workflow.[53] Co-crystalized ligands (native ligands) were kept, where available, but the rest of molecules that do not belong to proteins, including water molecules were deleted. Default settings were used to prepare final structures which assign bond orders, optimize proteins to address any overlapping hydrogens and minimize final structures at OPLS4 forcefield.[54]

Table 1
Inverse molecular docking results for the most potent compound **5g** and **5i**.

Target Enzymes	PDB ID	Docking Scores (kcal/mol)			RMSD Value
		Native Ligand	**5g**	**5i**	
PI3K	1E7V	−9.02	−6.82	−7.01	0.41
PKC alpha	4RA4	−9.28	−3.63	−4.25	1.75
PKC theta	5F9E	−13.42	−2.41	−5.31	0.20
P38 mapk	2ZB1	−9.92	−4.63	−4.87	0.41
JNK1	1UKI	−9.85	−4.00	−4.75	0.34
JNK-3	3TTI	−12.97	−4.60	−4.40	0.24
COX-1					
	4O1Z	−5.17	NP	NP	1.89
COX-2	3LN1	−11.53	NP	NP	0.25
NFkappaB p50[a]	1NFK	–	−4.01	−1.68	NA
Cjun/cfos[b]	1FOS	–	−1.24	−1.27	NA

NP: No poses found.
[a] Grid box for the binding site was set to 30 Å according to the literature.[73]
[b] Grid box for the binding site was set to 20 Å according to the literature.[74]

The active compounds **5g** and **5i** were also prepared by utilizing LigPrep[55] tool. All states at target pH (7.0 ± 2.0), tautomers and all possible conformations were prepared using this tool to cover larger 3D chemical space.

Using grid generation tool, binding sites of proteins were identified by taking native ligands as reference structure. For the proteins where the native ligand was not available, the receptor grid was set up and generated using key residues that were taking from literature. Binding site size for those proteins were adjusted according to the literature (see Table 1 footnotes).

Glide XP[56] module of Schrödinger at default settings was used in molecular docking of active compounds to the library of the prepared proteins.

The stability and dynamics of the docked complexes of the most potent compounds **5g** and **5i** were evaluated by molecular dynamics simulations employing Desmond Software[57] implemented in Schrödinger software.

System builder tool was used to prepare the systems first. Complexes were immersed in an orthorhombic box and solvated using simple point charge (SPC) solvent model.[58] Neutralization process was performed with sodium counterions and then 0.15 M NaCl was added. Final systems were subjected to the MD simulations for 200 ns with normal pressure (1.01325 bar) and temperature (300 K) (NPT) ensemble at default relaxation protocol. Recording interval was 200 ps that yielded about 1000 frames.

Molecular descriptors related to absorption, distribution, metabolism and excretion (ADME) analysis were calculated using QikProp of Schrödinger.[59]

2.7. Determination of acid dissociation constants

Potentiometric titrations were performed with the model TitroLine® 7000 automatic titrator using a combined glass electrode and pH values were measured. Standard buffer solutions pH 4.01, pH 7.00, and pH 10.01 were used when the glass electrode was calibrated according to the procedure described elsewhere.[60,61] For the potentiometric titrations, a double-walled glass titration cell with a thermostat at 25.0 ± 0.1 °C was used. During the titration, the titration cell was stirred at a constant rate using a magnetic stirrer, and high-purity nitrogen was

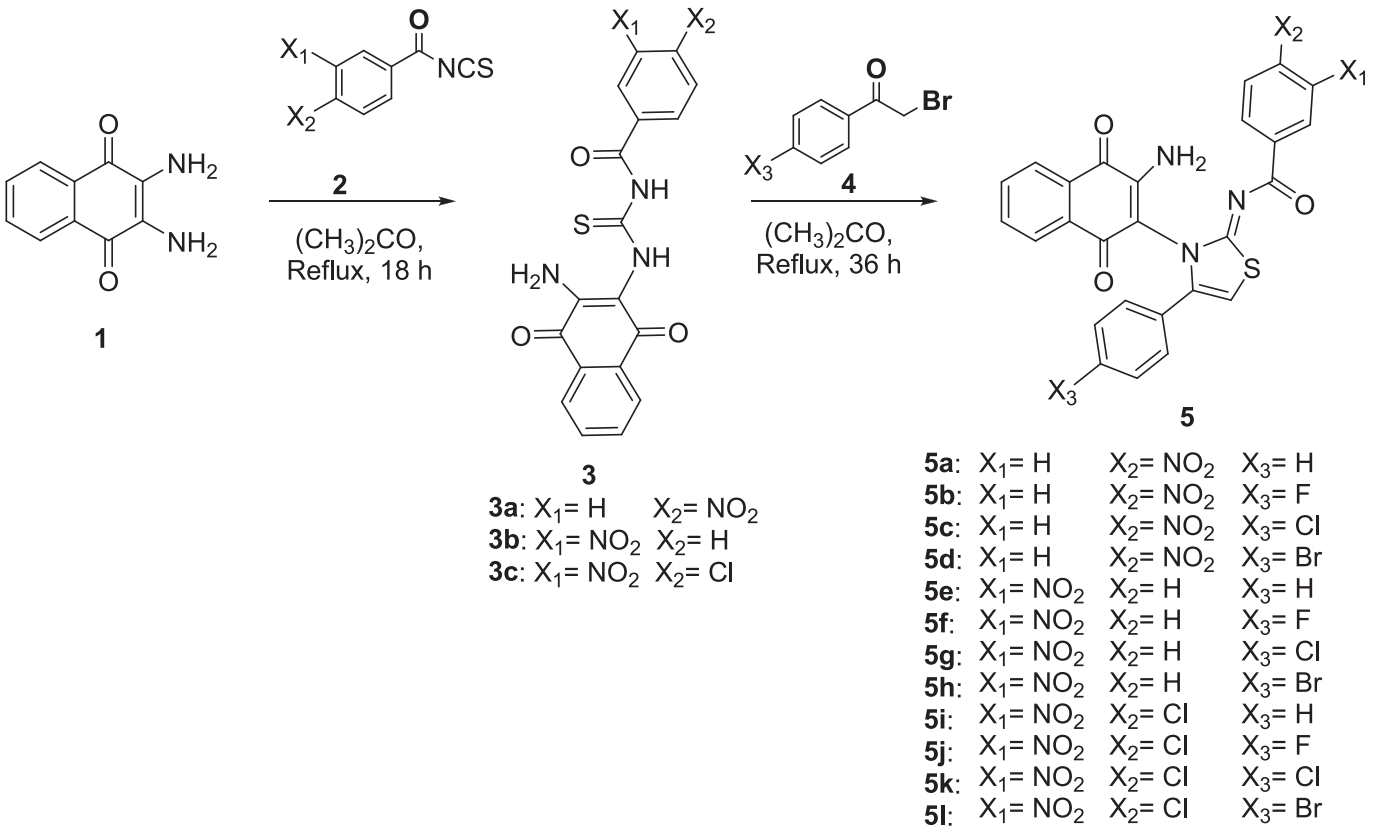

Scheme 1. Synthesis of the naphthoquinone-thiazole hybrids **5a–l**.

passed through the titration cell.

The stock solutions prepared for titration are as follows: Stock solutions of 1.10^{-3} M **5a–l** in DMSO, 0.025 M NaOH (used as titrant), 0.1 M HCl (used to obtain acidic medium), and 1.0 M NaCl (used to adjust ionic strength) in deionized water were prepared. To determine the pK_a values of **5a–l** in DMSO-water (20:80 v/v) in a dimethyl sulfoxide-water (20:80 v/v) solvent mixture at a 0.1 M NaCl ionic strength, titration cell was supplemented with 5 mL of the **5a–l** ligand solutions, 1 mL HCl and 5 mL NaCl solution from previously prepared stock solutions. Then, 5 mL of DMSO and 34 mL of deionized water were added to the titration cell. The pK_w value, which is defined as $-\log[H^+][OH^-]$ for the aqueous system, was obtained as 14.45 ± 0.05 at the ionic strength employed. pK_a values of **5a–l** were calculated with the HYPERQUAD computer program using the obtained potentiometric data.

3. Results and discussion

3.1. Synthesis and characterization

The naphthoquinone-thiazole hybrids **5a–l** were synthesized by the reaction of naphthoquinone acyl thiourea derivatives **3a–c** with various 2-bromo-1-substituted ethanones **4** in acetone under reflux temperature in 70–92 % yield. The preparation of naphthoquinone-thiazole hybrids as a result of the reactions between naphthoquinone acyl thiourea derivatives and 2-bromo-1-substituted ethanones and their stereochemistry determination were described in our previous study.[20] The naphthoquinone acyl thioureas **3a–c** used as intermediates were prepared according to a previous literature method[51] by reacting 2,3-dichloronaphthalene-1,4-dione **1** with corresponding acyl isothiocyanate **2** (Scheme 1). The molecular structures **5a–l** were characterized by ^{1}H NMR, ^{13}C NMR, FT-IR, HRMS, and elemental analysis (see supplementary part). The compounds **5a–d** were obtained in 24 h, the synthesis of **5e–h** was completed in 36 h and finally, the reaction time for **5i–l** was 72 h. In the ^{1}H NMR spectra of **5a–l**, the characteristic singlet peak of the thiazole ring proton was observed in the range of 7.25–7.32 ppm. Proton peaks of amine groups in **5a–l** were detected in different places since one proton forms hydrogen bonds with the benzamide moiety. It was observed that the carbon peak of the thiocarbonyl group in **3a–c** disappeared in the ^{13}C NMR spectra of the products **5a–l**. In the ^{13}C NMR spectra of **5a–l**, the carbon peaks of the three C=O carbons found in the molecular structures of the products were observed in the range of 180.9–169.9 ppm.

3.2. Cell viability

None of the compounds caused any cell death at all concentrations with and without LPS (Fig. 1). Hence, they might have the potential of being drug candidates compatible with the body that do not show cytotoxic properties to prevent the inflammatory reactions of immune cells. In the next phase of our study, we focused of the immunomodulatory properties of these compounds by measuring cytokine production levels of cells in the immune system. Depending on the results, they could be developed further to be used in autoimmune disorders with no cytotoxic properties.

The effect of 12 molecules on the production levels of two cytokines, TNF-α and IL6, were examined (Figs. 2–5). Comparison of TNF-α and IL6 cytokines with and without LPS was followed (Figs. 2–5). To examine the production levels of TNF-α and IL6 cytokines, 12 molecules were applied at concentrations of 1 μg /mL, 2 μg/mL, and 5 μg/mL.

No cytokine production was observed in the cells in the negative control group. LPS has a feature that stimulates the inflammatory reactions in macrophage cells. It's enhancing effect on TNF-α was observed. The LPS positive control group showed 8000 pg/mL for TNF-α. The TNF-α was decreased in LPS + SA compared to the LPS wells. The anti-inflammatory effect of LPS + SA was observed that by a decreased TNF-α concentration compared to the LPS control group (Figs. 2 and 3).

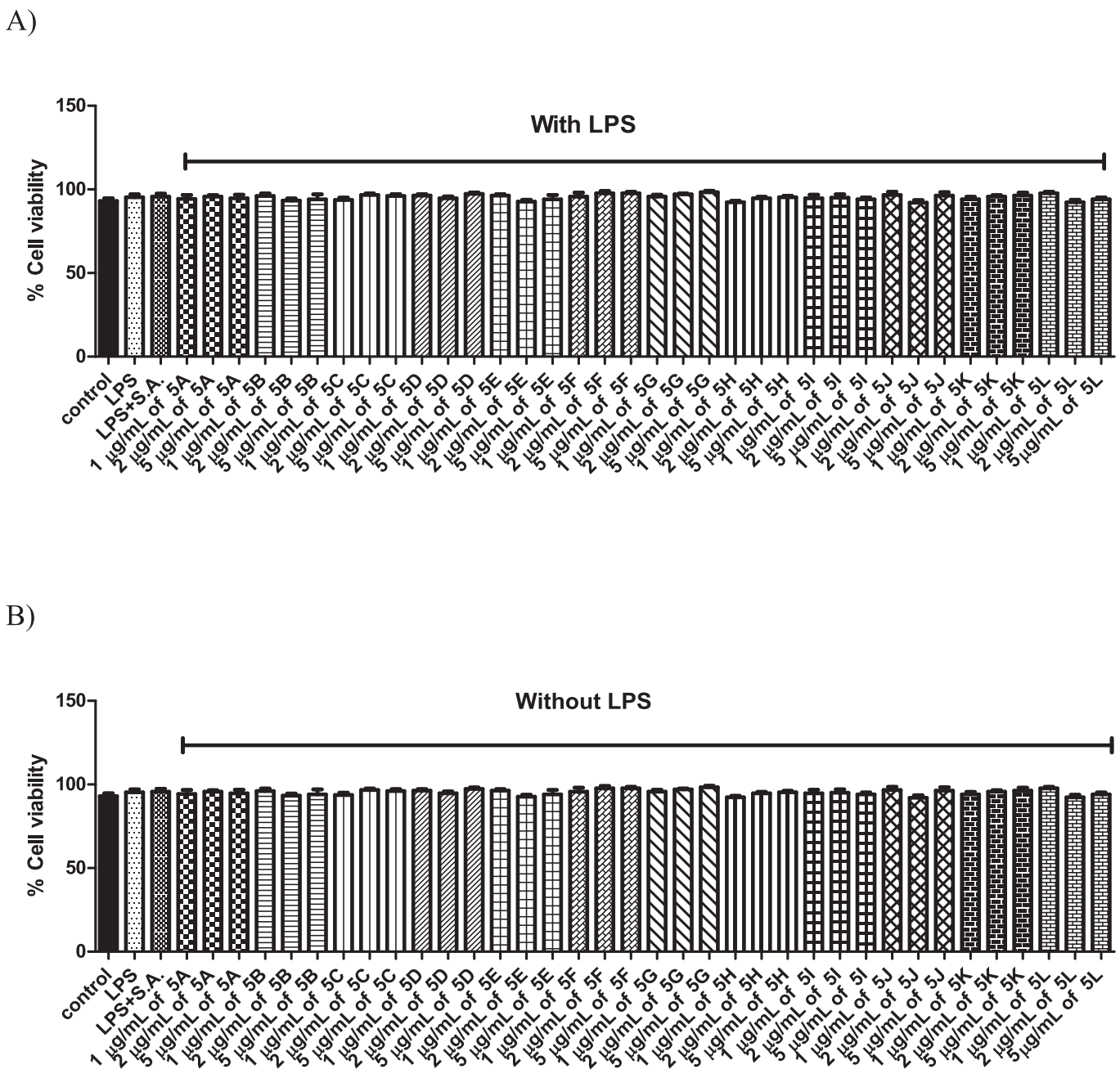

Fig. 1. After 1 day of incubation, the molecules used at concentrations of 1, 2, and 5 µg/mL were transferred into the wells with and without LPS to determine the cell viability. Immune cells of the J774.2 line were stimulated for 1 day with the molecules in the absence and presence of LPS. In the negative control group, 5 µg/mL SA was added. The cell viability was determined by using trypan blue. ***$p < 0.0001$, **$p < 0.0005$, *$p < 0.001$ ($N = 3$).

When the 3 different concentrations of the **5a** molecule were examined, no change was observed in the anti-inflammatory properties depending on the concentrations. However, anti-inflammatory effects of **5b**, **5c**, and **5d** were increased in parallel with the concentration levels by observing a reduction in TNF-α in the presence of LPS. On the other hand, compounds **5e** and **5g** had a greater effect on TNF-α at 5 µL/mL concentration (Fig. 2).

Production levels of 12 molecules our 2 cytokines, TNF α, and IL6, were examined without adding LPS. No effect on TNF-α was observed in the negative control group. In the LPS well, there was an increase in TNF-α production. There was a decrease in TNF-α production in LPS + SA wells compared to the LPS wells (Fig. 2). No production of TNF-α cytokine was detected in the presence of these 12 molecules alone (without LPS) (Fig. 3) meaning that there was no effect on the cytokine production by our molecules in the absence of LPS.

In the control group, there were no stimuli for IL6 production (Figs. 4 and 5). Therefore, IL6 production was not observed in the control group. Since LPS is known to have a stimulating effect on cytokine production of cells, the results obtained from the 12 substances used were interpreted in comparison to the data of the LPS group. Our negative control was SA and in the presence of SA, there was a decrease in IL6 production in LPS-stimulated cells compared to the LPS-treated group alone (Figs. 4 and 5). Thus, we can conclude that SA has an anti-inflammatory effect. There was no difference in IL6 production values at 1 and 2 µL/mL concentrations of **5e** (Fig. 4). The anti-inflammatory effect was higher at the concentration of 5 µL/mL. **5f** had a dose-dependent anti-inflammatory effect based on IL6 production levels (Fig. 4). There was no difference between the IL6 production levels in the **5g** molecule at

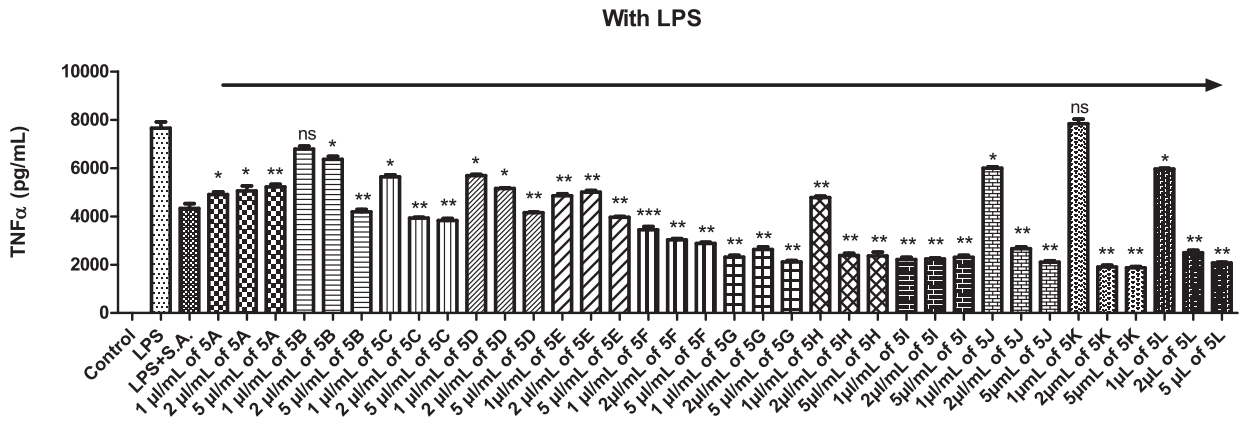

Fig. 2. After 1 day of incubation, the molecules used at 1, 2, and 5 μg/mL concentrations were transferred into the wells with LPS to determine the TNF production levels. Immune cells of the J774.2 line were stimulated for 1 day with the molecules in the absence and presence of LPS. In the negative control group 5 μg/mL SA was added. ELISA method was used to determine the TNF concentration. ***p < 0.0001, **p < 0.0005, *p < 0.001 (N = 3).

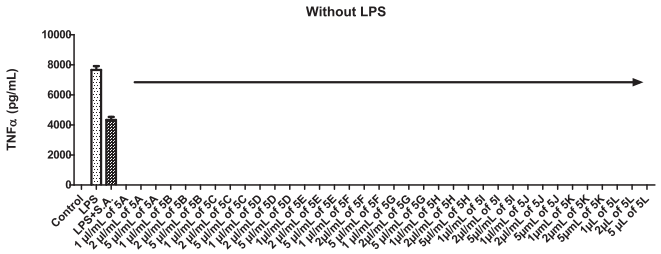

Fig. 3. After 1 day of incubation, the molecules used at 1, 2, and 5 μg/mL concentrations were transferred into the wells without LPS to determine the TNF production levels. Immune cells of the J774.2 line were stimulated for 1 day with the molecules in the absence and presence of LPS. In negative control group 5 μg/mL SA was added. ELISA method was used to determine the TNF concentration. ***p < 0.0001, **p < 0.0005, *p < 0.001 (N = 3).

concentrations of 2 and 5 μg/mL, but compared to LPS treated group alone it had anti-inflammatory activity (Fig. 4). It was observed that the anti-inflammatory effect was lower at 1 μL/mL concentration compared to other concentrations for **5g**, so there was a dose-dependent activity. **5h** and **5i** had anti-inflammatory activity independent of their doses (Fig. 4). **5j** exerted a dose-dependent anti-inflammatory activity for IL6 production levels (Fig. 4). No anti-inflammatory effect was observed at 1 μL/mL concentration of the **5k** molecule. But a stark anti-inflammatory effect was detected at 2 and 5 μL/mL concentrations (Fig. 4). The 1 μL/mL concentration of the **5k** molecule was the only concentration among all other molecules that did not show an anti-inflammatory effect. Among the 2 μL/mL concentrations in the graph, the molecule with the highest anti-inflammatory effect was the **5k** molecule. The anti-inflammatory effect increased as the concentration of **5l** increased (Fig. 4).

In the control group, no stimuli that could affect the production of IL6 cytokine were used (Fig. 5). Therefore, IL6 production was not observed in the control group. All compounds lacked immunostimulatory activity to produce IL6 in the absence of LPS (Fig. 5).

3.3. Inverse molecular docking and molecular dynamics simulations

In contrast to frequently used traditional molecular docking methods[62,63] which is the docking of a set of ligands to a specific target, we used inverse molecular docking protocol to predict possible target. Inverse docking is the docking of compounds to a library of receptors to identify potential targets. This approach has attracted much attention and has been successfully used as a novel technique in recent years.[64,65] We selected critical biological targets that, upon inhibition, could diminish expression of inflammatory mediators. PI3K, PKC, p38, JNK, COX, NFκB, and cJUN/cFos are pathways that have been associated with inflammatory responses by immune system cells. These pathways regulate cell survival, apoptosis, metabolism and gene expression that eventually alter the production rates of the inflammatory cytokines or mediators during an immune system response.[66–72] Therefore, they are major candidates for our molecular target analysis. In our study, we focused on the *in silico* analysis of the compounds for their potential

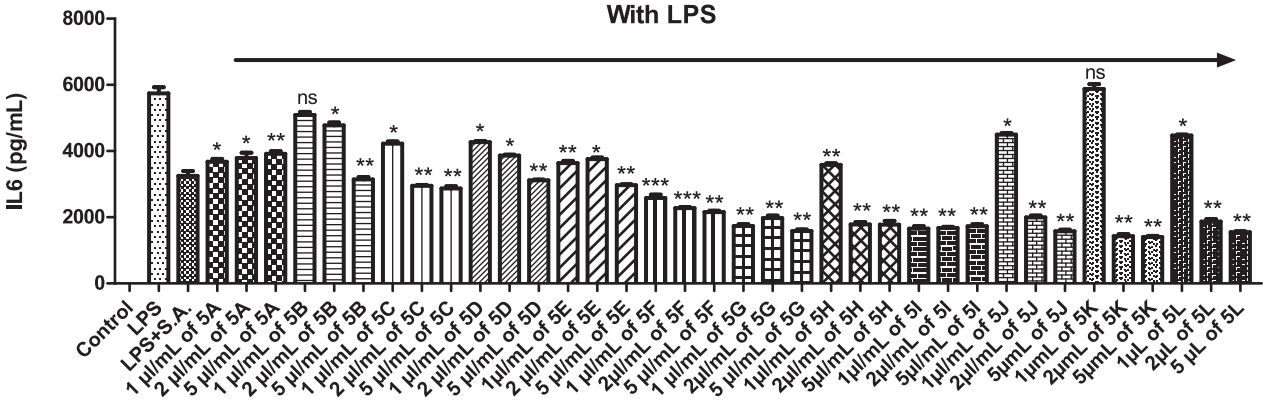

Fig. 4. After 1 day of incubation, the molecules used at of 1, 2, and 5 μg/mL concentrations were transferred into the wells with LPS to determine the IL6 production levels. Immune cells of the J774.2 line were stimulated for 1 day with the molecules in the absence and presence of LPS. In the negative control group, 5 μg/mL SA was added. ELISA method was used to determine the IL6 concentration. ***p < 0.0001, **p < 0.0005, *p < 0.001 (N = 3).

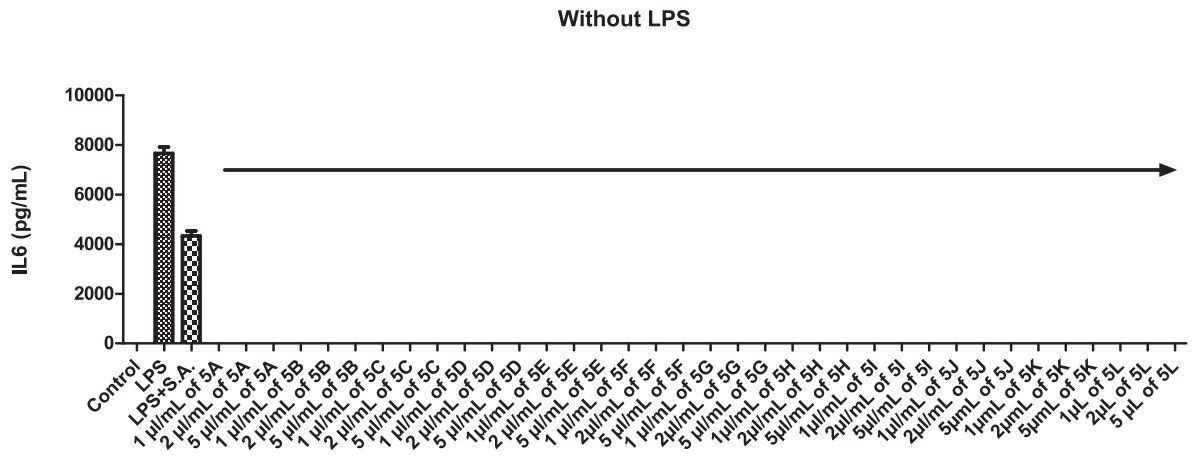

Fig. 5. After 1 day of incubation, the molecules used at 1, 2, and 5 μg/mL concentrations were transferred into the wells without LPS to determine the IL6 production levels. Immune cells of the J774.2 line were stimulated for 1 day with the molecules in the absence and presence of LPS. In the negative control group, 5 μg/mL SA was added. ELISA method was used to determine the IL6 concentration. ***$p < 0.0001$, **$p < 0.0005$, *$p < 0.001$ ($N = 3$).

interaction with these pathways.

As a critical step of molecular docking, root mean square deviation (RMSD) values were considered as internal validation of docking procedure which shows how well the software can reproduce x-ray crystal conformation of native ligand.[75] Glide XP with default settings was found to be successful for the target proteins. We identified PI3K as potential target based on the docking score threshold of −5.0 kcal/mol which was the lowest score predicted for the native ligands (Table 1). Besides that, Glide XP results reflected best for the most active compounds, **5g** and **5i**, against PI3K. Both compounds had the highest score for only PI3K.

The resulting docked complexes were then subjected to molecular dynamics simulations (200 ns) to predict stability of the complexes and most probable ligand interactions by analyzing simulation–interaction diagrams. Main graphs are given in Figs. 6 and 7. In both cases, the root mean square deviation (RMSD) values of proteins show slight deviations from their initial positions but remain under permissible thermal average of 1–3 Å which is an indication of a stable binding.[76] While protein ligand complex of **5i** was stable for whole time, protein-**5g** complex was stabilized after 75 ns of the simulation.

Ligand RMSD value of **5i** remained low that meant the ligand was not diffused away from the binding site of PI3K. Although **5g** seemed to undergo large conformational changes compared with its initial position, the variations were within the permissible range of ~3 Å during the whole course of simulation. Visual inspection of the simulation trajectories also confirmed that **5g** stayed in the binding pocket of PI3K.

The green vertical lines in RMSF graphs show the amino acids that the ligands are interacting with. For both compounds, the interacting residues have low RMSF values meaning that the ligands have favorable contacts which at the end, stabilize the whole system.

On the other hand, ligand-amino acid interactions that were lasted for at least one third of the simulation period were also evaluated. The noticeable interaction is the π-π interaction of **5g** with TYR867 that was stable for 92 % of all the simulation time. In addition, two more π-π stacking interaction were observed between **5g** and TRP812. Amino group of **5g** also engages in hydrogen bonding with ALA885 (46 %), VAL882 (68 %), LYS883 (70 %) and with ASP964 through water bridges. Walker *et al.*[77] reported detailed interactions of ATP and several inhibitors (wortmannin, LY294002, quercetin, myricetin, staurosporine) with PI3K. The discussion on the binding interactions will be based on this aforementioned study. One of the interactions in **5g**/PI3K complex is observed in the co-crystallized native ligand LY294002 which is a synthetic ligand that was reported to be much more stable PI3K inhibitor in solution than wortmannin. This interaction is the hydrogen bond with the backbone of VAL882 located at the hinge region and carbonyl oxygen of benzamide moiety of **5g**. Furthermore, the observed long-lasting interaction, hydrophobic π-π interaction with TYR867, is seen as a hydrogen bond in wortmannin/PI3K complex. Moreover, TRP812 is the same hydrophobic pocket that both LY294002 and wortmannin occupy. Although through water bridges, the interaction with ASP964 seems to be also vital because this amino acid involves in the binding of all inhibitors studied and also in ATP/enzyme complex. The most stable contact for **5i** is the π-cation bond between nitro group and TYR867 of PI3K that preserved for 73 % of MD simulation. Besides a hydrogen bond that formed between amino group and ASP950, **5i** exhibits two more hydrogen bonds with ALA885 and ASP964 via water bridges. Although none of those interactions are observed in the LY294002/PI3K complex, the hydrogen bond with TYR867 exists in wortmannin/PI3K and the amino acid residue ASP94 plays roles in the binding of all inhibitors reported as discussed above. In both compounds, aromatic rings, nitro and amino groups seem to be involved in most critical interactions.

Combination of experimental and *in silico* findings revealed that the presence of nitro group at X_1 position expressed a better activity. The strong electronegative atom, fluorine atom at position X_3 seemed to be detrimental to activity. As can be seen in Fig. 6, in such conformations, high electron density on both aromatic rings is crucial to engage in a *T*-shaped π-π interaction with the TRP812. If a ligand adopts in a different conformation as seen in **5i**, repulsion of negatively ionized amino acids residues such as ASP950 and ASP964 with fluorine end might result in an unfavourable conformation. This could be the reason that **5i** has better activity than **5b**.

It is of critical importance to take into account the ADME properties of compounds in the early stage of drug development. Therefore, a number of descriptors related to ADME were calculated for the compounds **5a–5i** (Table 2). Although majority of the compounds seems to violate one of the Lipinski's rule of five, this clearly results from molecular weights which are slightly >500. However, it is noteworthy to mention that those criteria are for orally absorbed drugs and not every oral drug obeys all those rules. For instance, many natural products are beyond the rule of five.[78] All compounds were predicted to have acceptable brain/blood partition coefficient which is important for central nervous system (CNS) targeted drugs. In addition, MDCK cells mimic for the blood–brain barrier and QPPMDCK parameters of the compounds also fall within acceptable ranges. QPlogPo/w values are around 3 that lie within acceptable range (2–4) for CNS penetration.[79] Thus, all compounds were predicted to have the ability to penetrate the blood–brain barrier. Caco-2 cells imitate gut-blood barrier. The QPPCaco values indicate that compounds might have good cell permeability *in vivo*. Overall descriptors in Table 2 show that our compounds

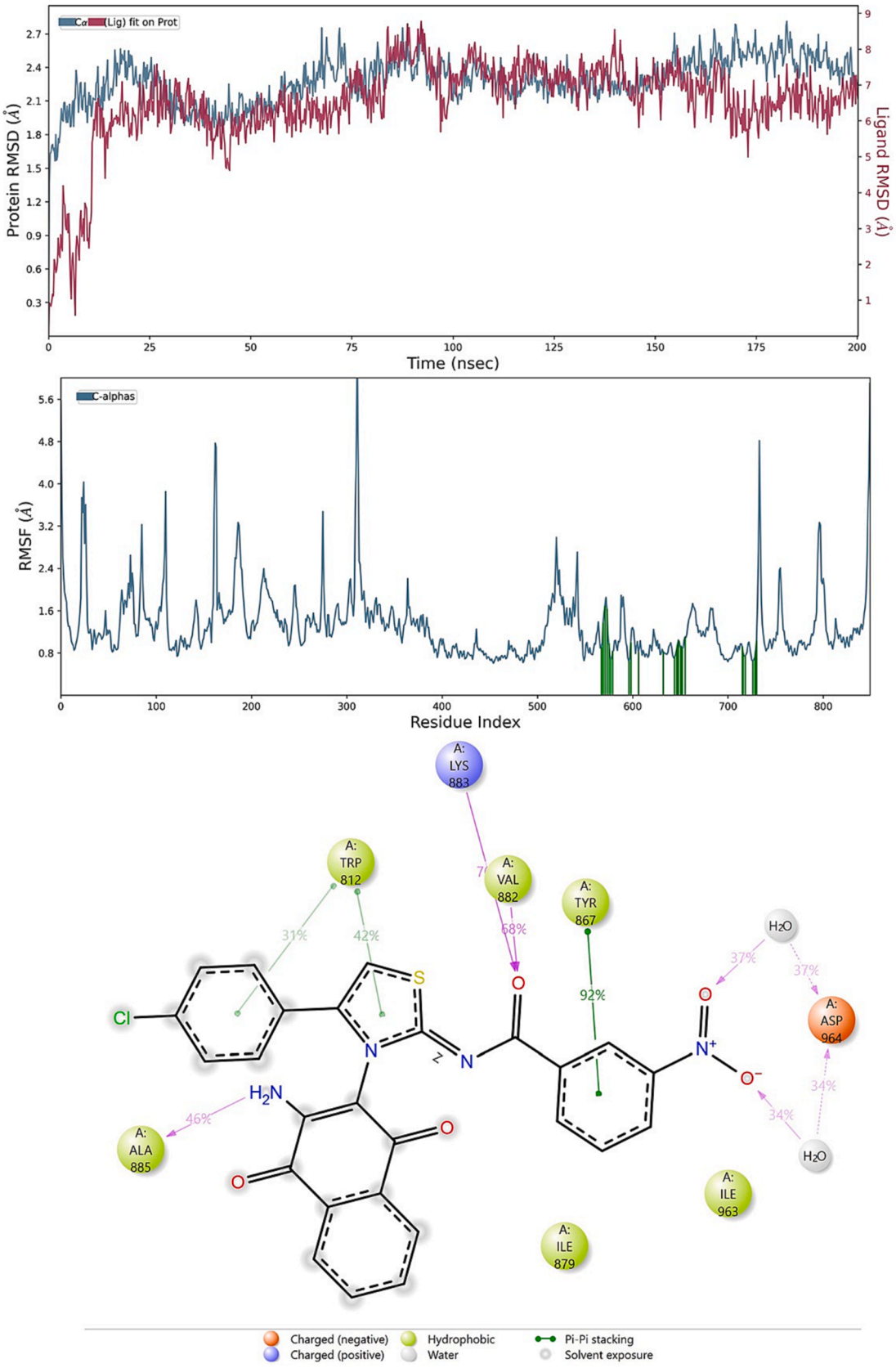

Fig. 6. Protein and ligand RMSD (top), RMSF (middle) and ligand–protein contact graphs for compound **5g**.

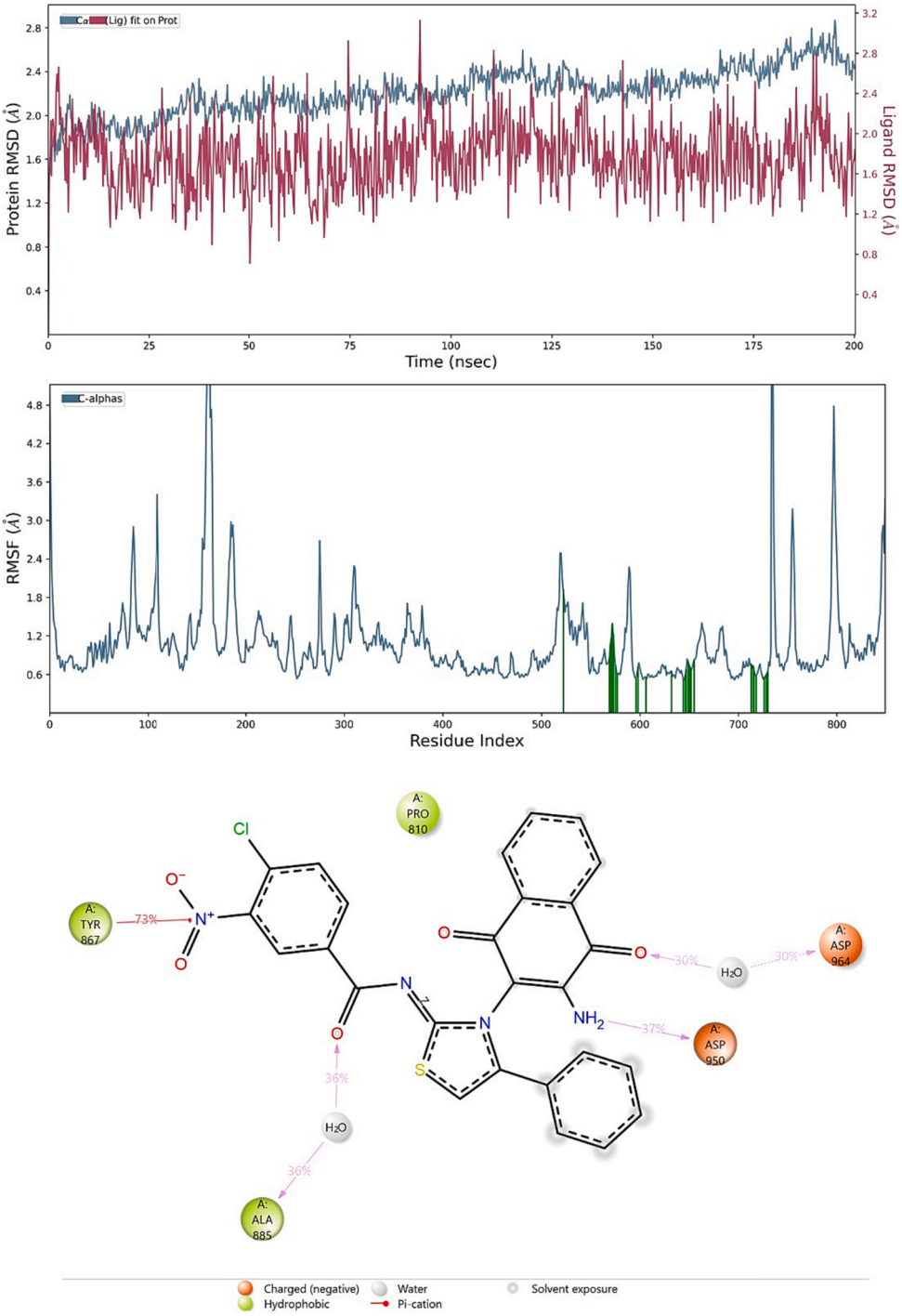

Fig. 7. Protein and ligand RMSD (top), RMSF (middle) and ligand–protein contact graphs for compound **5i**.

have good pharmacokinetic profiles and could be further developed as oral or parenteral drug candidates.

3.4. Acid dissociation constants

The pK_a values are one of the critical parameters that provide information about solubility and degree of ionization in various solvents and pH environments, as well as acidity/basicity and the hydrogen bonding capacity of the bioactive molecule. In addition, since drug molecules usually exhibit activity in ionized form, it is important to know the ionization state of each functional group in the drug molecule in its environment.[60,61] Because of the critical information that pK_a values give about the compounds, it is important to determine the pK_a values of the compounds. Since most organic compounds have low solubility in water and DMSO–water hydro-organic solvent systems provide significant advantages like compatibility with the standard glass electrode and a large acidity range, the DMSO–water mixture is widely used for the determination of potentiometrically pK_a values of organic compounds.[24,81]

The pK_a values of naphthoquinone thiazole hybrids **5a–l** were calculated by the HYPERQUAD computer program using data obtained potentiometrically at 25.0 ± 0.1 °C, 0.1 M ionic strength of NaCl in DMSO-water (20:80 *v/v*) hydro-organic solvent medium. Potentiometric titration studies were carried out according to the method specified in

Table 2
Calculated ADME related molecular properties of compounds **5a–l**.

Comp.	MW[a]	QPlogPo/w[b]	QPlogBB[c]	QPPMDCK[d]	PSA[e]	QPPCaco[f]	QPlogS[g]	%HOA[h]	RO5[i]
5a	496.50	3.19	−2.09	38.34	155.71	58.86	−5.93	77.27	0
5b	514.49	3.42	−2.00	68.38	155.72	58.20	−6.29	65.57	1
5c	530.94	3.67	−1.97	93.42	155.71	58.23	−6.66	67.05	1
5d	575.39	3.74	−1.97	100.30	155.72	58.16	−6.77	67.48	1
5e	496.50	3.30	−1.71	72.01	155.63	105.25	−5.54	82.47	0
5f	514.49	3.52	−1.76	100.10	155.62	82.66	−6.05	68.91	1
5g	530.94	3.78	−1.58	176.33	155.59	104.67	−6.24	72.25	1
5h	575.39	3.85	−1.57	189.98	155.63	104.80	−6.35	72.69	1
5i	530.94	3.77	−1.59	159.28	154.84	107.85	−6.18	72.42	1
5j	548.93	4.00	−1.49	287.88	154.85	107.94	−6.54	73.78	1
5k	565.39	4.25	−1.46	391.63	154.88	107.55	−6.91	75.23	1
5l	609.84	4.33	−1.45	425.32	154.84	108.53	−7.03	75.78	1

[a] Molecular weight (Recommended value: 130.0–725.0).
[b] Predicted octanol/water partition coefficient (recommended range: −2.0 to 6.5).
[c] Predicted brain/blood partition coefficient (recommended range: −3.0 to 1.2).
[d] Predicted apparent MDCK cell permeability in nm/sec (<25 poor, >500 great).
[e] Polar surface area (recommended range: 7.0 to 200.0).
[f] Predicted apparent Caco-2 cell permeability in nm/sec (<25 poor, >500 great).
[g] Predicted aqueous solubility (recommended range: −6.5 to 0.5).
[h] Percentage of human oral absorption (<25 % is weak and > 80 % is strong).
[i] Number of violations of Lipinski's rule of five[80] (maximum is 4).

Table 3
PK_a values of **5a–l** DMSO:water 20:80 *v/v*, 25.0 ± 0.1 °C, I = 0.1 M by NaCl.

Ligand	pK_{a1}	pK_{a2}	pK_{a3}	pK_{a4}
5a	2.58 ± 0.10	5.96 ± 0.07	7.06 ± 0.07	10.02 ± 0.04
5b	2.63 ± 0.12	5.95 ± 0.09	7.02 ± 0.08	10.03 ± 0.05
5c	2.96 ± 0.11	5.99 ± 0.09	6.95 ± 0.09	10.02 ± 0.06
5d	2.74 ± 0.10	5.99 ± 0.08	6.89 ± 0.08	9.98 ± 0.05
5e	3.00 ± 0.09	6.07 ± 0.07	6.96 ± 0.06	10.03 ± 0.03
5f	2.91 ± 0.11	6.10 ± 0.05	6.91 ± 0.05	10.02 ± 0.04
5g	2.92 ± 0.10	6.15 ± 0.07	7.02 ± 0.07	9.99 ± 0.05
5h	–	5.92 ± 0.11	7.29 ± 0.10	10.04 ± 0.06
5i	3.21 ± 0.11	6.12 ± 0.08	7.14 ± 0.08	9.97 ± 0.05
5j	3.05 ± 0.09	6.08 ± 0.07	7.08 ± 0.06	10.03 ± 0.04
5k	3.10 ± 0.11	6.10 ± 0.08	7.17 ± 0.08	10.03 ± 0.05
5l	2.98 ± 0.12	6.47 ± 0.08	–	10.03 ± 0.05

the literature.[82] The obtained pK_a values of **5a–l** are given in Table 3, and titration curves of **5a–d** and the distribution curve of compound **5a** for symbolizing all of the compounds **5a–l** are presented in Figures 8A and 8B, respectively. The titration curves of **5e–h** (Fig. S49A), **5i–l** (Fig. S49B), and the distribution curve of all compounds **5b–l** (Fig. S50) are presented in supplementary material.

In the experimental conditions performed, four pK_a values for **5a–g**, **5i–k**, and three pK_a values for **5h**, **5l** could be determined. Remarkably, all compounds have acidic character which is in agreement with the literature that non-steroidal anti-inflammatory drugs are strong organic acids with pK_as in the range of 3–5.[83] The pK_{a1}, pK_{a2}, pK_{a3}, and pK_{a4} values of naphthoquinone thiazole hybrids **5a–l** were found in a range of 2.58–3.21, 5.92–6.47, 6.89–7.29, and 9.97–10.04, respectively (Table 3). The pK_a value of the imino nitrogen atom of various Schiff bases containing a thiazole ring was reported to be in the range of 2.46–2.85.[84] Moreover, Öğretir et al.[85] reported that the pK_a value of the protonated thiazole nitrogen atom of various thiazoles in the imino form was in the range of 4.16–3.36 in the ethanol–water mixture. Aromatic amines such as aniline (pK_a = 1.02–6.08) have an acidic character[60,86], and similarly, the NH_2 group attached to the naphthoquinone structure is expected to have an acidic character. In addition, aromatic alcohols such as phenol (pK_a > 8[87]) have a basic character. Due to delocalization in the ring, the 1,4-naphthoquinone core can be considered as a naphthalene-1,4-diol core[88] and is expected to have a basic character similar to aromatic alcohols. In light of this information, it can say that

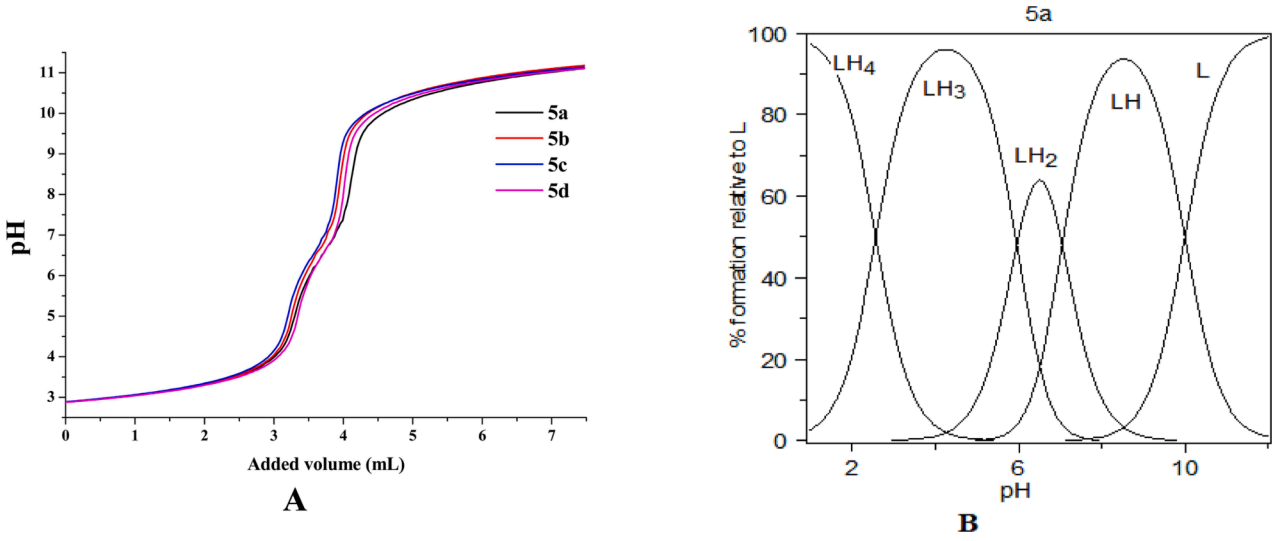

Fig. 8. (A) Titration curves of **5a–d** (25.0 ± 0.1 °C, I = 0.1 M by NaCl in DMSO:water, 20:80 *v/v*). (B) Distribution curve of **5a** for symbolized all of the products.

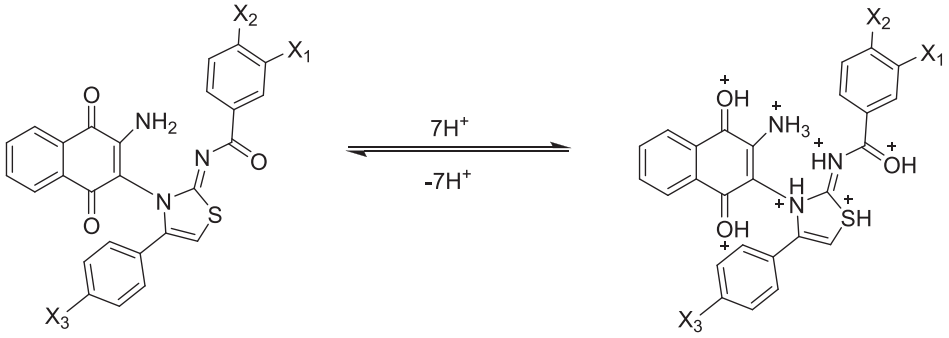

Fig. 9. The full protonated form of the prepared compounds **5a–l** (LH_7^{7+}).

the pK_{a1}, pK_{a2}, pK_{a3}, and pK_{a4} may be related to protonated imino nitrogen (C═N^+), amine (—NH_3^+), sulphur atom of the thiazole ring (SH^+), and one of the carbonyl oxygen atom (OH^+) of naphthoquinone core, respectively.

According to the results obtained by the HYPERQUAD program, four protonated species were obtained as LH, LH_2, LH_3, and LH_4 for **5a–g** and **5i–k**, and three protonated species were obtained as LH, LH_2, and LH_3 for **5h** and **5l** ligands. The full protonated form of the prepared compounds **5a–l** is shown in Fig. 9.

4. Conclusion

The synthesis of twelve new naphthoquinone thiazole hybrids was performed and their anti-inflammatory activities were investigated. These molecules were found to be potent immunomodulatory drug candidates that could suppress suppress the production of pro-inflammatory cytokines TNF-α and IL-6. The most potent compounds were further investigated *in silico* for their potential interaction with major signaling pathways that have important roles in inflammatory reactions. Inverse molecular docking approach was employed for the identification of potential target protein(s). Consequently, PI3K was predicted to be potential target enzyme that could be the possible mechanism of action. Subsequent molecular dynamics simulations confirmed stability of docked complexes and enlighten binding interactions at molecular level. All compounds were predicted to have good pharmacokinetic profiles. Finally, pK_a values of compounds that have critical roles in further pharmacological studies are also reported.

Declaration of Competing Interest

The authors declare that they have no known competing financial interests or personal relationships that could have appeared to influence the work reported in this paper.

Data availability

Data will be made available on request.

Acknowledgements

The authors thank The Scientific and Technological Research Council of Turkey (TÜBİTAK, project grant 118Z407) for financial support.

Appendix A. Supplementary material

Supplementary data to this article can be found online at https://doi.org/10.1016/j.bmc.2023.117510.

References

1. Zhang L, Zhang G, Xu S, Song Y. Recent advances of quinones as a privileged structure in drug discovery. *Eur J Med Chem*. 2021;223, 113632. https://doi.org/10.1016/j.ejmech.2021.113632.
2. Alrooqi M, Khan S, Alhumaydhi FA, et al. A therapeutic journey of pyridine-based heterocyclic compounds as potent anticancer agents: a review (From 2017 to 2021). *Anticancer Agents Med Chem*. 2022;22:2775–2787. https://doi.org/10.2174/1871520622666220324102849.
3. Devi M, Kumar P, Singh R, et al. A comprehensive review on synthesis, biological profile and photophysical studies of heterocyclic compounds derived from 2, 3-diamino-1, 4-naphthoquinone. *J Mol Struct*. 2022, 133786.
4. Yadav P, Kaushik CP, Kumar M, Kumar A. Phthalimide/naphthalimide containing 1,2,3-triazole hybrids: synthesis and antimicrobial evaluation. *J Mol Struct*. 2023: 1276. https://doi.org/10.1016/j.molstruc.2022.134688.
5. Aminin D, Polonik S. 1,4-Naphthoquinones: some biological properties and application. *Chem Pharm Bull (Tokyo)*. 2020;68:46–57. https://doi.org/10.1248/cpb.c19-00911.
6. Li K, Wang B, Zheng L, et al. Target ROS to induce apoptosis and cell cycle arrest by 5,7-dimethoxy-1,4-naphthoquinone derivative. *Bioorg Med Chem Lett*. 2018;28: 273–277. https://doi.org/10.1016/j.bmcl.2017.12.059.
7. Morris A, Hoyle R, Pagare PP, et al. Exploration of naphthoquinone analogs in targeting the TCF-DNA interaction to inhibit the Wnt/β-catenin signaling pathway. *Bioorg Chem*. 2022;124, 105812. https://doi.org/10.1016/j.bioorg.2022.105812.
8. Mohamady S, Gibriel AA, Ahmed MS, Hendy MS, Naguib BH. Design and novel synthetic approach supported with molecular docking and biological evidence for naphthoquinone-hydrazinotriazolothiadiazine analogs as potential anticancer inhibiting topoisomerase-IIB. *Bioorg Chem*. 2020;96, 103641. https://doi.org/10.1016/j.bioorg.2020.103641.
9. Nural Y, Ozdemir S, Doluca O, et al. Synthesis, biological properties, and acid dissociation constant of novel naphthoquinone–triazole hybrids. *Bioorg Chem*. 2020; 105, 104441. https://doi.org/10.1016/j.bioorg.2020.104441.
10. Erasmus C, Aucamp J, Smit FJ, et al. Synthesis and comparison of in vitro dual anti-infective activities of novel naphthoquinone hybrids and atovaquone. *Bioorg Chem*. 2021;114, 105118. https://doi.org/10.1016/j.bioorg.2021.105118.
11. Riaz MT, Yaqub M, Shafiq Z, et al. Synthesis, biological activity and docking calculations of bis-naphthoquinone derivatives from Lawsone. *Bioorg Chem*. 2021; 114, 105069. https://doi.org/10.1016/j.bioorg.2021.105069.
12. Cabral RG, Viegas G, Pacheco R, Sousa AC, Robalo MP. Sustainable synthesis, antiproliferative and acetylcholinesterase inhibition of 1,4- and 1,2-naphthoquinone derivatives. *Molecules*. 2023;28:1232. https://doi.org/10.3390/molecules28031232.
13. Abdullah Al Awadh A. Biomedical applications of selective metal complexes of indole, benzimidazole, benzothiazole and benzoxazole: a review (From 2015 to 2022). Saudi Pharm J 2023;31(9):101698. doi: 10.1016/j.jsps.2023.101698.
14. Kurt AH, Ayaz L, Ayaz F, Seferoglu Z, Nural Y. A review on the design, synthesis, and structure-activity relationships of benzothiazole derivatives against hypoxic tumors. *Curr Org Synth*. 2022;19:772–796. https://doi.org/10.2174/1570179419666220330001036.
15. Sadgir NV, Adole VA, Dhonnar SL, Jagdale BS. Synthesis and biological evaluation of coumarin appended thiazole hybrid heterocycles: antibacterial and antifungal study. *J Mol Struct*. 2023;1293, 136229. https://doi.org/10.1016/j.molstruc.2023.136229.
16. Lengerli D, Ibis K, Nural Y, Banoglu E. The 1,2,3-triazole 'all-in-one' ring system in drug discovery: a good bioisostere, a good pharmacophore, a good linker, and a versatile synthetic tool. *Expert Opin Drug Discov*. 2022;17:1209–1236. https://doi.org/10.1080/17460441.2022.2129613.
17. Jaismy Jacob P, Manju SL. Novel approach of multi-targeted thiazoles and thiazolidenes toward anti-inflammatory and anticancer therapy—dual inhibition of COX-2 and 5-LOX enzymes. *Med Chem Res*. 2021;30:236–257. https://doi.org/10.1007/s00044-020-02655-9.
18. Singh A, Malhotra D, Singh K, Chadha R, Bedi PMS. Thiazole derivatives in medicinal chemistry: recent advancements in synthetic strategies, structure activity relationship and pharmacological outcomes. *J Mol Struct*. 2022;1266, 133479. https://doi.org/10.1016/j.molstruc.2022.133479.

19. Jagadale SM, Abhale YK, Pawar HR, et al. Synthesis of new thiazole and pyrazole clubbed 1,2,3-triazol derivatives as potential antimycobacterial and antibacterial agents. *Polycycl Aromat Compd*. 2022;42:3216–3237. https://doi.org/10.1080/10406638.2020.1857272.
20. Gemili M, Nural Y, Keleş E, et al. Novel highly functionalized 1,4-naphthoquinone 2-iminothiazole hybrids: synthesis, photophysical properties, crystal structure, DFT studies, and anti(myco)bacterial/antifungal activity. *J Mol Struct*. 2019;1196:536–546. https://doi.org/10.1016/j.molstruc.2019.06.087.
21. Nural Y, Gemili M, Yabalak E, De Coen LM, Ulger M. Green synthesis of highly functionalized octahydropyrrolo[3,4-c]pyrrole derivatives using subcritical water, and their anti(myco)bacterial and antifungal activity. Arkivoc 2018:51–64. doi: 10.24820/ark.5550190.p010.573.
22. Svirčev M, Popsavin M, Pavić A, et al. Design, synthesis, and biological evaluation of thiazole bioisosteres of goniofufurone through in vitro antiproliferative activity and in vivo toxicity. *Bioorg Chem*. 2022;121, 105691. https://doi.org/10.1016/j.bioorg.2022.105691.
23. Donarska B, Świtalska M, Płaziński W, Wietrzyk J, Łączkowski KZ. Effect of the dichloro-substitution on antiproliferative activity of phthalimide-thiazole derivatives. Rational design, synthesis, elastase, caspase 3/7, and EGFR tyrosine kinase activity and molecular modeling study. *Bioorg Chem*. 2021;110, 104819. https://doi.org/10.1016/j.bioorg.2021.104819.
24. Doğan A, Özdemir S, Yalçın MS, Sarı H, Nural Y. Naphthoquinone–thiazole hybrids bearing adamantane: synthesis, antimicrobial, DNA cleavage, antioxidant activity, acid dissociation constant, and drug-likeness. J Res Pharm 2021;25(3):292–304. doi: 10.29228/jrp.20.
25. Fayed EA, Ragab A, Ezz Eldin RR, Bayoumi AH, Ammar YA. In vivo screening and toxicity studies of indolinone incorporated thiosemicarbazone, thiazole and piperidinosulfonyl moieties as anticonvulsant agents. *Bioorg Chem*. 2021;116, 105300. https://doi.org/10.1016/j.bioorg.2021.105300.
26. Mor S, Khatri M. Synthesis, antimicrobial evaluation, α-amylase inhibitory ability and molecular docking studies of 3-alkyl-1-(4-(aryl/heteroaryl)thiazol-2-yl)indeno[1,2-c]pyrazol-4(1H)-ones. *J Mol Struct*. 2022;1249, 131526. https://doi.org/10.1016/j.molstruc.2021.131526.
27. Osmaniye D, Görgülü Ş, Sağlık BN, Levent S, Özkay Y, Kaplancıklı ZA. Design, synthesis, in vitro and in silico studies of some novel thiazole-dihydrofuran derivatives as aromatase inhibitors. *Bioorg Chem*. 2021;114, 105123. https://doi.org/10.1016/j.bioorg.2021.105123.
28. Alzahrani AY, Ammar YA, Abu-Elghait M, et al. Development of novel indolin-2-one derivative incorporating thiazole moiety as DHFR and quorum sensing inhibitors: synthesis, antimicrobial, and antibiofilm activities with molecular modelling study. *Bioorg Chem*. 2022;119, 105571. https://doi.org/10.1016/j.bioorg.2021.105571.
29. Medzhitov R. Origin and physiological roles of inflammation. *Nature*. 2008;454:428–435. https://doi.org/10.1038/nature07201.
30. Della Valle A, Dimmito MP, Zengin G, et al. Exploring the nutraceutical potential of dried pepper *Capsicum annuum* L. on market from Altino in Abruzzo Region. Antioxidants 2020;9(5):400. doi: 10.3390/antiox9050400.
31. Efeoglu C, Yetkin D, Nural Y, Ece A, Seferoğlu Z, Ayaz F. Novel urea-thiourea hybrids bearing 1, 4-naphthoquinone moiety: anti-inflammatory activity on mammalian macrophages by regulating intracellular PI3K pathway, and molecular docking study. *J Mol Struct*. 2022;1264, 133284.
32. Mezeiova E, Janockova J, Andrys R, et al. 2-Propargylamino-naphthoquinone derivatives as multipotent agents for the treatment of Alzheimer's disease. *Eur J Med Chem*. 2021;211, 113112. https://doi.org/10.1016/j.ejmech.2020.113112.
33. Kapoor N, Kandwal P, Sharma G, Gambhir L. Redox ticklers and beyond: Naphthoquinone repository in the spotlight against inflammation and associated maladies. *Pharmacol Res*. 2021;174, 105968. https://doi.org/10.1016/j.phrs.2021.105968.
34. Mahmoud IS, Hatmal MM, Abuarqoub D, et al. 1,4-Naphthoquinone Is a potent inhibitor of IRAK1 kinases and the production of inflammatory cytokines in THP-1 differentiated macrophages. *ACS Omega*. 2021;6:25299–25310. https://doi.org/10.1021/acsomega.1c03081.
35. Bawazeer S, Rauf A. In vivo anti-inflammatory, analgesic, and sedative studies of the extract and naphthoquinone isolated from *Diospyros kaki* (Persimmon). *ACS Omega*. 2021;6:9852–9856. https://doi.org/10.1021/acsomega.1c00537.
36. Liu H, Yan C, Li C, You T, She Z. Naphthoquinone derivatives with anti-inflammatory activity from mangrove-derived endophytic fungus *Talaromyces* sp. SK-S009. *Molecules*. 2020;25(3):576. https://doi.org/10.3390/molecules25030576.
37. Kumar G, Singh NP. Synthesis, anti-inflammatory and analgesic evaluation of thiazole/oxazole substituted benzothiazole derivatives. *Bioorg Chem*. 2021;107, 104608. https://doi.org/10.1016/j.bioorg.2020.104608.
38. Zhang Z, Cao P, Fang M, et al. Design, synthesis, and SAR study of novel 4,5-dihydropyrazole-Thiazole derivatives with anti-inflammatory activities for the treatment of sepsis. *Eur J Med Chem*. 2021;225, 113743. https://doi.org/10.1016/j.ejmech.2021.113743.
39. Abdel-Aziz SA, Taher ES, Lan P, et al. Design, synthesis, and biological evaluation of new pyrimidine-5-carbonitrile derivatives bearing 1,3-thiazole moiety as novel anti-inflammatory EGFR inhibitors with cardiac safety profile. *Bioorg Chem*. 2021;111, 104890. https://doi.org/10.1016/j.bioorg.2021.104890.
40. Modrić M, Božičević M, Faraho I, Bosnar M, Škorić I. Design, synthesis and biological evaluation of new 1,3-thiazole derivatives as potential anti-inflammatory agents. *J Mol Struct*. 2021;1239, 130526. https://doi.org/10.1016/j.molstruc.2021.130526.
41. Jacob PJ, Manju SL. Identification and development of thiazole leads as COX-2/5-LOX inhibitors through in-vitro and in-vivo biological evaluation for anti-inflammatory activity. *Bioorg Chem*. 2020;100, 103882. https://doi.org/10.1016/j.bioorg.2020.103882.
42. Maghraby MTE, Abou-Ghadir OMF, Abdel-Moty SG, Ali AY, Salem OIA. Novel class of benzimidazole-thiazole hybrids: the privileged scaffolds of potent anti-inflammatory activity with dual inhibition of cyclooxygenase and 15-lipoxygenase enzymes. *Bioorg Med Chem*. 2020;28, 115403. https://doi.org/10.1016/j.bmc.2020.115403.
43. Ahmed A, Molvi KI, Patel HM, Ullah R, Bari A. Synthesis of novel 2, 3, 5-tri-substituted thiazoles with anti-inflammatory and antibacterial effect causing clinical pathogens. *J Infect Public Health*. 2020;13:472–479. https://doi.org/10.1016/j.jiph.2020.02.002.
44. Lomba LA, Vogt PH, Souza VEP, et al. A naphthoquinone from *Sinningia canescens* inhibits inflammation and fever in mice. *Inflammation*. 2017;40:1051–1061. https://doi.org/10.1007/s10753-017-0548-y.
45. Wongrakpanich S, Wongrakpanich A, Melhado K, Rangaswami J. A comprehensive review of non-steroidal anti-inflammatory drug use in the elderly. *Aging Dis*. 2018;9:143. https://doi.org/10.14336/AD.2017.0306.
46. Fujiwara N, Kobayashi K. Macrophages in inflammation. *Curr Drug Target -Inflamm Allergy*. 2005;4:281–286. https://doi.org/10.2174/1568010054022024.
47. Zhang C, Yang M, Ericsson AC. Function of macrophages in disease: current understanding on molecular mechanisms. *Front Immunol*. 2021:12. https://doi.org/10.3389/fimmu.2021.620510.
48. Önal HT, Yetkin D, Ayaz F. Escitalopram's inflammatory effect on the mammalian macrophages and its intracellular mechanism of action. *Prog Neuropsychopharmacol Biol Psychiatry*. 2023;125, 110762. https://doi.org/10.1016/j.pnpbp.2023.110762.
49. Yetkin D, Yılmaz İA, Ayaz F. Anti-inflammatory activity of bupropion through immunomodulation of the macrophages. *Naunyn Schmiedebergs Arch Pharmacol*. 2023;396:2087–2093. https://doi.org/10.1007/s00210-023-02462-0.
50. Batu Öztürk A, Can Öztürk N, Ayaz F. Conditioned media of mouse macrophages modulates neuronal dynamics in mouse hippocampal cells. *Int Immunopharmacol*. 2023;114, 109548. https://doi.org/10.1016/j.intimp.2022.109548.
51. Nural Y, Karasu E, Keleş E, et al. Synthesis of novel acylthioureas bearing naphthoquinone moiety as dual sensor for high-performance naked-eye colorimetric and fluorescence detection of CN− and F− ions and its application in water and food samples. *Dyes Pigm*. 2022;198, 110006.
52. Schrödinger. Schrödinger. In (Version 2023-2). Published online 2023. New York, NY: Schrödinger, LLC.
53. Schrödinger. Protein Preparation Wizard. In (Version 2023-2). Published online 2023: New York, NY: Schrödinger, LLC.
54. Lu C, Wu C, Ghoreishi D, et al. OPLS4: Improving force field accuracy on challenging regimes of chemical space. *J Chem Theory Comput*. 2021;17. https://doi.org/10.1021/acs.jctc.1c00302.
55. Schrödinger. LigPrep. In: In (Version 2023-2). New York, NY: Schrödinger, LLC; 2023.
56. Friesner RA, Murphy RB, Repasky MP, et al. Extra precision glide: docking and scoring incorporating a model of hydrophobic enclosure for protein-ligand complexes. *J Med Chem*. 2006;49. https://doi.org/10.1021/jm051256o.
57. Schrödinger. Desmond Molecular Dynamics System. In (Version 2023-2). Published online 2023. D. E. Shaw Research, New York, NY: Maestro-Desmond.
58. Mark P, Nilsson L. Structure and dynamics of the TIP3P, SPC, and SPC/E water models at 298 K. *Chem A Eur J*. 2001;105. https://doi.org/10.1021/jp003020w.
59. Schrödinger. QikProp. In (Version 2023-2). Published online 2023. New York: Schrödinger, LLC.
60. Nural Y. Synthesis, antimycobacterial activity, and acid dissociation constants of polyfunctionalized 3-[2-(pyrrolidin-1-yl)thiazole-5-carbonyl]-2H-chromen-2-one derivatives. *Monatshefte für Chemie - Chem Monthly*. 2018;149:1905–1918.
61. Nural Y, Ozdemir S, Yalcin MS, et al. New bis- and tetrakis-1,2,3-triazole derivatives: synthesis, DNA cleavage, molecular docking, antimicrobial, antioxidant activity and acid dissociation constants. *Bioorg Med Chem Lett*. 2022;55, 128453. https://doi.org/10.1016/j.bmcl.2021.128453.
62. Başoğlu F, Ulusoy-Güzeldemirci N, Akalın-Çiftçi G, Çetinkaya S, Ece A. Novel imidazo[2,1-b]thiazole-based anticancer agents as potential focal adhesion kinase inhibitors: synthesis, in silico and in vitro evaluation. *Chem Biol Drug Des*. 2021;98. https://doi.org/10.1111/cbdd.13896.
63. Chan K, Frankish N, Zhang T, et al. Bioactive indanes: insight into the bioactivity of indane dimers related to the lead anti-inflammatory molecule PH46A. *J Pharm Pharmacol*. 2020;72. https://doi.org/10.1111/jphp.13269.
64. Priyanca Devi A, Ameta KL, Alshehri S, et al. Pharmacokinetics of some newly synthesized 1, 5- benzothiazepine scaffolds: a molecular docking and molecular dynamics simulation approach. *J King Saud Univ Sci*. 2023;35. https://doi.org/10.1016/j.jksus.2022.102528.
65. Kores K, Kolenc Z, Furlan V, Bren U. Inverse molecular docking elucidating the anticarcinogenic potential of the hop natural product xanthohumol and its metabolites. *Foods*. 2022;11. https://doi.org/10.3390/foods11091253.
66. Koyasu S. The role of PI3K in immune cells. *Nat Immunol*. 2003;4:313–319. https://doi.org/10.1038/ni0403-313.
67. Lim PS, Sutton CR, Rao S. Protein kinase C in the immune system: from signalling to chromatin regulation. *Immunology*. 2015;146:508–522. https://doi.org/10.1111/imm.12510.
68. Cook R, Wu CC, Kang YJ, Han J. The role of the p38 pathway in adaptive immunity. *Cell Mol Immunol*. 2007;4.
69. Huang G, Shi LZ, Chi H. Regulation of JNK and p38 MAPK in the immune system: signal integration, propagation and termination. *Cytokine*. 2009;48:161–169. https://doi.org/10.1016/j.cyto.2009.08.002.
70. Liu B, Qu L, Yan S. Cyclooxygenase-2 promotes tumor growth and suppresses tumor immunity. *Cancer Cell Int*. 2015;15:106. https://doi.org/10.1186/s12935-015-0260-7.

71. Liu T, Zhang L, Joo D, Sun SC. NF-κB signaling in inflammation. *Signal Transduct Target Ther*. 2017;2:17023. https://doi.org/10.1038/sigtrans.2017.23.
72. Hop HT, Arayan LT, Huy TXN, et al. The key role of c-Fos for immune regulation and bacterial dissemination in Brucella infected macrophage. *Front Cell Infect Microbiol*. 2018:8. https://doi.org/10.3389/fcimb.2018.00287.
73. Piccagli L, Fabbri E, Borgatti M, et al. Docking of molecules identified in bioactive medicinal plants extracts into the p50 NF-kappaB transcription factor: correlation with inhibition of NF-kappaB/DNA interactions and inhibitory effects on IL-8 gene expression. *BMC Struct Biol*. 2008:8. https://doi.org/10.1186/1472-6807-8-38.
74. El-Banna AA, Darwish RS, Ghareeb DA, Yassin AM, Abdulmalek SA, Dawood HM. Metabolic profiling of *Lantana camara* L. using UPLC-MS/MS and revealing its inflammation-related targets using network pharmacology-based and molecular docking analyses. *Sci Rep*. 2022;12. https://doi.org/10.1038/s41598-022-19137-0.
75. Ece A. Computer-aided drug design. *BMC Chem*. 2023;17:1. https://doi.org/10.1186/s13065-023-00939-w.
76. Güleç Ö, Türkeş C, Arslan M, et al. Novel beta-lactam substituted benzenesulfonamides: in vitro enzyme inhibition, cytotoxic activity and in silico interactions. J Biomol Struct Dyn 2023:1–19. doi: 10.1080/07391102.2023.2240889.
77. Walker EH, Pacold ME, Perisic O, et al. Structural determinants of phosphoinositide 3-kinase inhibition by Wortmannin, LY294002, quercetin, myricetin, and staurosporine. *Mol Cell*. 2000;6:909–919. https://doi.org/10.1016/S1097-2765(05)00089-4.
78. Doak BC, Over B, Giordanetto F, Kihlberg J. Oral druggable space beyond the rule of 5: insights from drugs and clinical candidates. *Chem Biol*. 2014;21:1115–1142. https://doi.org/10.1016/j.chembiol.2014.08.013.
79. Hitchcock SA, Pennington LD. Structure–brain exposure relationships. *J Med Chem*. 2006;49:7559–7583. https://doi.org/10.1021/jm060642i.
80. Lipinski CA, Lombardo F, Dominy BW, Feeney PJ. Experimental and computational approaches to estimate solubility and permeability in drug discovery and development settings. *Adv Drug Deliv Rev*. 1997;23:3–25. https://doi.org/10.1016/S0169-409X(96)00423-1.
81. Nural Y, Gemili M, Seferoglu N, Sahin E, Ulger M, Sari H. Synthesis, crystal structure, DFT studies, acid dissociation constant, and antimicrobial activity of methyl 2-(4-chlorophenyl)-7a-((4-chlorophenyl)carbamothioyl)-1-oxo-5,5-diphenyl-3-thioxo-hexahydro-1H-pyrrolo[1,2-e]imidazole-6-carboxylate. *J Mol Struct*. 2018;1160:375–382. https://doi.org/10.1016/j.molstruc.2018.01.099.
82. Nural Y, Ozdemir S, Yalcin MS, et al. Synthesis, biological evaluation, molecular docking, and acid dissociation constant of new bis-1, 2, 3-triazole compounds. *ChemistrySelect*. 2021;6:6994–7001.
83. Asirvatham S, Dhokchawle BV, Tauro SJ. Quantitative structure activity relationships studies of non-steroidal anti-inflammatory drugs: a review. *Arab J Chem*. 2019;12:3948–3962. https://doi.org/10.1016/j.arabjc.2016.03.002.
84. Altun Y, Köseoğlu F, Demirelli H, Yılmaz İ, Çukurovalı A, Kavak N. Potentiometric studies on nickel (II), copper (II) and zinc (II) metal complexes with new schiff bases containing cyclobutane and thiazole groups in 60 % dioxane-water mixture. *J Braz Chem Soc*. 2009;20:299–308. https://doi.org/10.1590/S0103-50532009000200015.
85. Öğretir C, Demirayak Ş, Duran M. Spectroscopic determination and evaluation of acidity constants for some drug precursor 2-amino-4-(3- or 4-substituted phenyl) thiazole derivatives. *J Chem Eng Data*. 2010;55:1137–1142. https://doi.org/10.1021/je9005739.
86. Gross KC, Seybold PG. Substituent effects on the physical properties and pKa of aniline. *Int J Quantum Chem*. 2000;80:1107–1115.
87. Gross KC, Seybold PG. Substituent effects on the physical properties and pKa of phenol. *Int J Quantum Chem*. 2001;85:569–579. https://doi.org/10.1002/qua.1525.
88. Chiang Y, Kresge AJ, Hellrung B, Schünemann P, Wirz J. Flash photolysis of 5-methyl-1,4-naphthoquinone in aqueous solution: kinetics and mechanism of photoenolization and of enol trapping. *Helv Chim Acta*. 1997;80:1106–1121. https://doi.org/10.1002/hlca.19970800408.